X N8400049

NEANDC (E) - 242 U Vol. V
INDC (Ger) - 25/L + Special
FIZ-KA--6

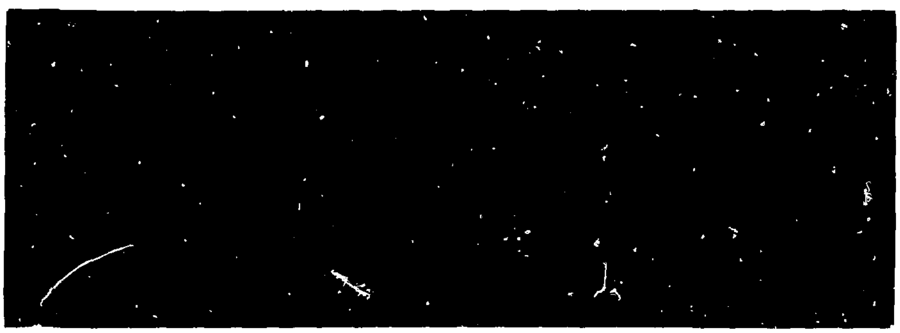

Fachinformationszentrum
Energie
Physik
Mathematik

ISSN 0172-2204
1983
Nr. 6

NEANDC (E) - 242 U Vol. V
INDC (Ger) - 25/L + Special
FIZ-KA--6

PROGRESS REPORT
ON NUCLEAR DATA RESEARCH IN THE FEDERAL REPUBLIC OF GERMANY

for the Period April 1, 1982 to March 31, 1983

June 1983

Edited by
S. Cierjacks
Kernforschungszentrum Karlsruhe
Institut für Kernphysik
and
H. Behrens
Fachinformationszentrum Energie
Physik, Mathematik, Karlsruhe

FACHINFORMATIONSZENTRUM ENERGIE · PHYSIK · MATHEMATIK GMBH KARLSRUHE

November 1983, Nr. 6 ISSN 0172-2204

Vertrieb:

Fach-
informations-
zentrum

Energie
Physik
Mathematik GmbH
Karlsruhe

7514 Eggenstein-Leopoldshafen 2
Telefon (07247) 824600/01
Telex 7826487 fize d

Preis: 14,70 DM (incl. MwSt.) + Porto

Printed in the Federal Republic of Germany

Druck:
Druckhaus Karlsruhe GmbH
Ostring 6
7500 Karlsruhe 1

Foreword

This report has been prepared to promote exchange of nuclear data research information between the Federal Republic of Germany and the other member states of NEA and IAEA. It brings together progress reports from KfK Karlsruhe, KFA Jülich, the Universities of Hamburg, Kiel, Köln, Mainz, Marburg, München and Stuttgart, as well as from PTB Braunschweig and FIZ Karlsruhe. The emphasis in the work reported here has been on measurement, evaluation and compilation of application-oriented nuclear data, such as those relevant to fission and fusion reactor technologies, development of intense spallation neutron sources, production of medically important short-lived radioisotopes, etc.

Each contribution is presented under the laboratory heading where the work was done. If the work is relevant to requests in the World Request List for Nuclear Data, WRENDA 79/80 (INDC (SEC) - 73/URSF), the corresponding request identification numbers have been listed after the title and authors' names of the respective contribution.

Karlsruhe, June 1983

S. Cierjacks
H. Behrens

C O N T E N T S

Page

KERNFORSCHUNGSZENTRUM KARLSRUHE
INSTITUT FÜR ANGEWANDTE KERNPHYSIK

KERNFORSCHUNGSZENTRUM KARLSRUHE

INSTITUT FÜR ANGEWANDTE KERNPHYSIK

1. 3 MV Van de Graaff-Accelerator

1.1 Isotopic Neon Cross Sections for a Study of Neutron Balance and Temperature During s-Process Nucleosynthesis*

J. Almeida+ and F. Käppeler

The neutron source of the s-process is believed to be the $^{22}Ne(\alpha,n)$ reaction, taking place in the He-burning shell of a pulsating red giant. Such a periodic neutron irradiation leads to an exponential distribution of neutron fluences for the seed nuclei, which can be deduced from the observed solar system abundances. Using this empirically determined distribution of neutron fluences and the abundances and the cross sections of the elements present in the He shell, the number of neutrons captured by each nuclear species during the s-process has been calculated. The ^{22}Ne has as progenitors the C, N, and O isotopes involved in the CNO cycle, and is the most abundant nuclear species (apart from ^{4}He and ^{12}C) in the He shell; it was therefore anticipated that it would be a major neutron absorber. We have thus measured the capture cross sections of the three stable neon isotopes in the energy range 5-400 keV, and we determined the 30 keV Maxwellian averaged cross section with an accuracy of better than 1 mb; the total cross sections were also measured, between 5 and 800 keV.

As a result it was found that the $^{22}Ne(\alpha,n)$ reaction can indeed satisfy the neutron balance condition that as many neutrons should be produced as are absorbed. From this condition we conclude that at least 80 % of the ^{22}Ne must undergo the (α,n) reaction, which implies that less than 20 % can undergo the (α,γ) reaction. Therefore, neutron absorption by the light elements, from ^{20}Ne to ^{56}Fe, is dominated not by ^{22}Ne, but by ^{25}Mg which is produced abundantly by the $^{22}Ne(\alpha,n)$ reaction. The reaction rate ratio $^{22}Ne(\alpha,n)/^{22}Ne(\alpha,\gamma)$ derived from the neutron balance condition allows an estimate of the s-process temperature T, via the energy dependence of these rates. We obtain a lower limit $T_s > 3.2 \times 10^8$ K or $kT_s > 27$ keV, consistent with the temperature of the He-burnung shell.

* The Astrophysical Journal, 265;417 (1983)

+ LNETI - DEEN, Est.Nac. 10, 2685 Sacavem, Portugal

1.2 Neutron Capture Resonances in ^{56}Fe and ^{58}Fe in the Energy Range from 10 to 100 keV*

F. Käppeler, K. Wisshak, and L. D. Hong

(Relevant to request numbers: 692101, 692103, 692104, 714005, 741040, 753036, 762100, 792201, 741046, 691104, 762179)

The neutron capture cross section of ^{56}Fe and ^{58}Fe has been measured in the energy range form 10 to 250 keV relative to the gold standard. A pulsed 3 MV Van de Graaff accelerator and the $^{7}Li(p,n)$ reaction served as a neutron source. Capture gamma rays were detected by two C_6D_6 detectors, which were operated in coincidence and anticoincidence mode. Two-dimensional data acquisition allowed to apply the pulse height weighting technique off-line. The samples were located at a flight path of 60 cm. The total time resolution was 1.2 ns thus allowing for an energy resolution of 2 ns/m. The experimental set-up was optimized with respect to low background and low neutron sensitivity. The additional flight path of 4 cm from the sample to the detector was sufficient to discriminate capture of sample scattered neutrons by the additional time of flight. In this way reliable results were obtained even for the strong s-wave resonances of both isotopes. The experimental capture yield was analyzed with the FANAC code. The energy resolution allowed to extract resonance parameters in the energy range from 10 to 100 keV. The individual systematic uncertainties of the experimental method are discussed in detail. They were found to range between 5 and 10 % while the statistical uncertainty is 3-5 % for most of the resonances. A comparison to the results of other authors exhibits in case of ^{56}Fe systematic differences of 7-11 %. For ^{58}Fe the present results differ up to 50 % from the only other measurement for this isotope.

---

* KfK-Report 3412 and Nucl. Sci. Eng. in print

1.3 Neutron Capture in s-Wave Resonances of ^{56}Fe, ^{58}Ni, ^{60}Ni*

K. Wisshak, F. Käppeler, G. Reffo+, and F. Fabbri+

(Relevant to request numbers: 762074, 692101, 692103, 692104, 714005, 741040, 753036, 762100, 792201, 761039, 741046, 692128, 692131, 702009, 741053, 753039, 762110, 792207, 792010, 741056, 741059)

The neutron capture widths of s-wave resonances in ^{56}Fe (27.7 keV), ^{58}Ni(15.4 keV) and ^{60}Ni (12.5 keV) have been determined using a setup completely different from previous experiments. A pulsed 3-MV Van de Graaff accelerator and a kinematically collimated neutron beam, produced via the ^{7}Li(p,n) reaction, was used in the experiments. Capture gamma-rays were observed by three Moxon-Rae detectors with graphite-, bismuth-graphite-, and bismuth-converters, respectively. The samples were positioned at a neutron flight path of only 8 cm. Thus events due to capture of resonance scattered neutrons in the detectors or in surrounding materials are completely discriminated by their additional time of flight. The high neutron flux at the sample position allowed the use of very thin samples (0.15 mm - 0.45 mm), avoiding large multiple scattering corrections. The data obtained with the individual detectors were corrected for the efficiency of the respective converter materials. For that purpose, detailed theoretical calculations of the capture gamma-ray spectra of the measured isotopes and of gold, which was used as a standard, were performed. The final results are: Γ_γ(27.7 keV, ^{56}Fe) = 1.06 $\pm$ 0.05 eV, Γ_γ(15.4 keV, ^{58}Ni) = 1.53 $\pm$ 0.10 eV and Γ_γ(12.5 keV, ^{60}Ni) = 2.92 $\pm$ 0.19 eV. The accuracy obtained with the present experimenental method represents an improvement of a factor 3-6 compared to previous experiments. The investigated s-wave resonances contribute 10 - 40 % to the total capture rate of the respective isotopes in a typical fast reactor.

---

* KfK-Report 3516 and submitted for publ. to Nucl. Sci. Eng.

+ Energia Nucleare et Energia Alternativa, Bologna, Italy

1.4 Neutron Capture in s-Wave Resonances of ^{64}Ni

K. Wisshak, F. Käppeler, R.L. Macklin[+], and G. Reffo[++]

(Relevant to request number 741068)

The neutron capture widths of s-wave resonances in ^{64}Ni at 13.9 and 33.8 keV have been determined. As Γ_n/Γ_γ is 2900 and 7740 for these resonances, respectively, accurate results can be obtained only using a setup with extremely low neutron sensitivity completely different from all previous experiments. A pulsed 3-MV Van de Graaff accelerator and a kinematically collimated neutron beam, produced via the ^{7}Li(p,n) reaction, was used in the experiments. Capture gamma-rays were observed by three Moxon-Rae detectors with graphite-, bismuth-graphite-, and bismuth-converters, respectively. The samples were positioned at a neutron flight path of only 6-8 cm. Thus events due to capture of resonance scattered neutrons in the detectors or in surrounding materials are completely discriminated by their additional time of flight. The short flight path and the high neutron flux at the sample position allowed for a signal to background ratio of $\sim$ 1 even for the broad resonance at 33.8 keV. The data obtained with the individual detectors were corrected for the efficiency of the respective converter materials. For that purpose, detailed theoretical calculations of the capture gamma-ray spectra of the measured isotopes and of gold, which was used as a standard, were performed. The preliminary results are Γ_γ(13.9 keV) = 1.00 eV and Γ_γ(33.8 keV) = 1.15 eV. This is considerably less than the rough estimates obtained for these resonances in previous work. The overall statistical and systematic uncertainty is not yet finally analyzed but will be of the order of 10 %.

In Fig. 1 FANAC fits to the experimental capture yield are shown for three different runs performed with modified experimental conditions. The dashed line represents the contribution of the s-wave resonance at 33.8 keV, the dotted line is due to capture in isotopic impurities.

+ Oak Ridge National Laboratory, Oak Ridge, Tenn., USA

++ Energia Nucleare et Energia Alternativa, Bologna, Italy

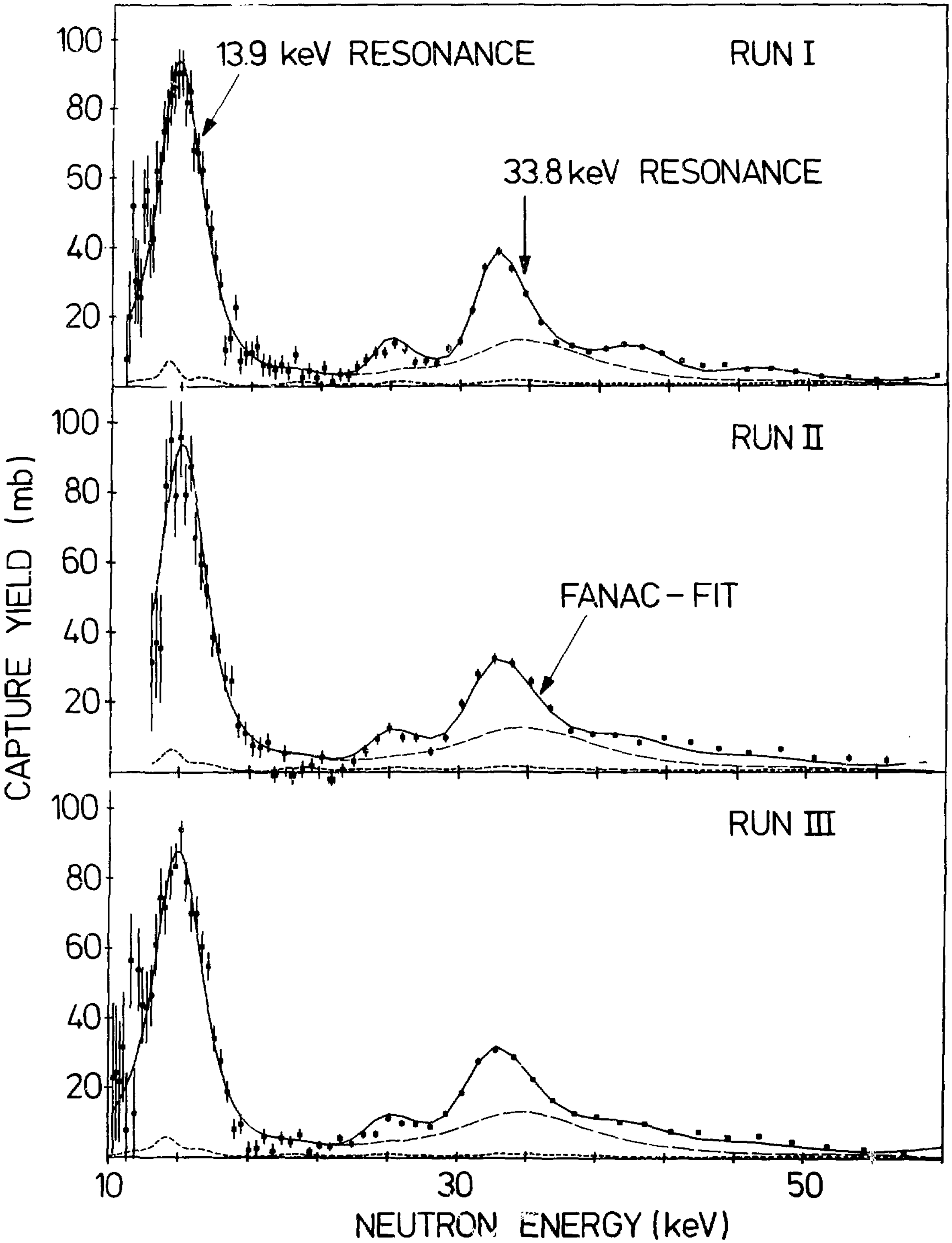

Fig. 1 FANAC fits to the capture yield of ^{64}Ni as obtained in three different runs with modified experimental conditions.

1.5 Neutron Capture Cross Section of ^{80}Kr for $4 \leq E_n \leq 290$ keV

G. Walter, F. Käppeler, Z. Y. Bao[+]

We have measured the $^{80}Kr(n,\gamma)\,^{81}Kr$ cross section for neutron energies reaching from 4 to 290 keV relative to the standard cross section of ^{197}Au.

Capture events were registered by detecting the gamma-ray cascade from the deexciting compound nucleus with two C_6D_6-scintillators. Neutron energies were determined by time-of-flight. With an overall time resolution of $\sim$ 1 ns and a flight path of 60.5 cm we obtained an energy resolution of $\sim$ 0.5 keV at 30 keV neutron energy, most of this being due to the 20 mm diameter of the high pressure gas sphere used as a sample.

From our data we calculated the Maxwellian average of the capture cross section for kT = 30 keV which is needed for the analysis of the s-process branching at ^{79}Se in astrophysics. We found $\langle\sigma(^{80}Kr)\rangle = 257 \pm 12$ mb.

+ Inst. of Atomic Energy, Beijing Peoples Rep. of China

1.6 The Chemical Fixation of Kr isotopes in Zeolite 5 A. - Prerequisite for the Determination of 25 keV Neutron Capture Cross Sections with the Activation Method.[+]

R.-D. Penzhorn, G. Walter, H. Beer

By chemical fixation of Kr in zeolite 5 A adequate samples can be obtained to determine the capture cross section of reactions such as $^{84}Kr(n,\gamma)\,^{85}Kr^m$ and $^{86}Kr(n,\gamma)\,^{87}Kr$. The employed zeolite loading was of the order 52 - 66 {cm³ STP Kr / g zeolite}. The capture cross section of the reaction $^{84}Kr(n,\gamma)\,^{85}Kr^m$ was determined at thermal and 25 keV neutron energy. The value obtained at 25 keV is of relevance to the stellar nucleosynthesis of heavy elements.

+ accepted for publ. in Zeitschrift für Naturforschung

1.7 Neutron Capture Cross Sections at 25 keV by the Activation Method

G. Walter and H. Beer

The Maxwellian averaged neutron capture cross sections of ^{71}Ga, ^{75}As, $^{79,81}Br$, ^{86}Kr and $^{85,87}Rb$ have been measured at $kT = 25$ keV by activation relative to the standard ^{197}Au.

Neutrons were produced by the reaction $^{7}Li(p,n)^{7}Be$ 25 keV above the reaction threshold, the energy spectrum being almost Maxwellian (deviation $\sim$ 3 %) for the chosen experimental set-up.

After activation the induced activities were counted in subsequent time intervals via a strong characteristic γ line with a γx-Germanium detector (45 cm^3, energy resolution at 1.33 MeV: 1.6 keV).

These cross sections are applied to nuclear astrophysics in analysing the synthesis of heavy elements by the s-process.

1.8 Neutron Capture Cross Sections of the Stable Xenon Isotopes and Their Application in Stellar Nucleosynthesis

H. Beer, F. Käppeler and G. Reffo+
(Relevant to request mumbers: 752014N,801277R,812038N,812039N)

The neutron capture cross sections of $^{124,132,134}Xe$ have been measured by the activation technique at 25 keV neutron energy. These data were supplemented by calculated capture cross sections for $^{128,129,130,131}Xe$ via the statistical model. The complete set of capture cross sections obtained in this way served to determine the solar xenon abundance through s-process systematics and to study a variety of isotopic anomalies.

+ E.N.E.A. Bologna, Italy

1.9 Neutron Capture Cross Section of $^{142,143,144}Nd$

G. J. Mathews+, F. Käppeler

The Nd isotopes are abundant fission products and therefore of interest for the reactor neutron balance. At the same time the keV cross section (especially that of ^{142}Nd) are important for nuclear astrophysics. Mainly for the second reason we have remeasured the capture cross sections of $^{142,143,144}Nd$ between 6 and 250 keV neutron energy. The experimental set-up consisted of two C_6D_6 detectors with off-line pulse height weighting. Neutrons were produced at the Karlsruhe Van de Graaff accelerator via the $^7Li(p,n)$-reaction. A flight path of 0.60 m and an overall time resolution of $\sim$ 1.2 ns allowed for a resolution of $\Delta E/E$ = 300 eV at 30 keV. Our results for the 30 keV Maxwellian averaged cross section are shown in Table I together with previous data.

Table I 30-keV Maxwellian Averaged Cross Sections (mb)

Isotope	Ko 78	Mu 78	Na 79	this work
^{142}Nd	48 $\pm$ 8	57 $\pm$ 7		62.5 $\pm$ 5.3
^{143}Nd		265 $\pm$ 50	319 $\pm$ 26	298 $\pm$ 29
^{144}Nd		65 $\pm$ 10		154 $\pm$ 7

Ko 78 V.N. Kononov et al., Sov. J. Nucl. Phys. 27 (1978) 5

Mu 78 A.R. de L. Musgrove et al., Proc. Int. Conf. on Neutron Physics and Nuclear Data, Harwell p. 449 (1979)

Na 79 Y. Nakajima et al., Proc. Int. Conf. on Neutron Physics and Nuclear Data, Harwell p. 438 (1979)

We find good agreement with existing measurements for all isotopes but for ^{144}Nd where a severe discrepancy of more than a factor 2 shows up. This cross section may therefore deserve further attention.

+ Univ. of California, Lawrence Livermore Laboratory, Livermore Calif. 94550 USA

1.10 $^{148,150}Sm$: A Test for s-Process Nucleosynthesis

R.R. Winters[+], F. Käppeler, K. Wisshak, G. Reffo[++], and A. Mengoni[++]
(Relevant to request numbers: 752019N, 801280R, 792226R, 752020N, 801281R, 752021R, 792225R, 801282R)

The odd Sm isotopes exhibit large capture cross sections and are at the same time abundant fission products. Beside their resulting impact on the neutron balance at higher burn-up, the long lived $^{151}Sm(t_{1/2}$=93a) contributes to the long term hazard of HAW. This cross section of ^{151}Sm has not been measured so far and therefore it was important to collect reliable information on the cross sections systematics of neighboring nuclei.

In the field of nuclear astrophysics there is complementary interest in the even isotopes $^{148,150}Sm$ which allow to check the striking prediction of the s-process theory of nucleosynthesis, namely that the product $(\sigma_{n\gamma} \cdot N_s)$ should be nearly equal for neighboring s-only isotopes.

Such tests using isotopes of Te and Ba verified the prediction with an uncertainty of 10 - 15 %. Discrepant results from previous measurements of the neutron capture cross section of ^{150}Sm, however, confused the situation.

For these reasons we have remeasured $\sigma_{n,\gamma}$ for $^{148,149,150}Sm$ in the energy range from 4 - 250 keV giving careful attention to reducing systematic errors.

Table I Experimental values for the 30 keV Maxwellian Averaged Cross Sections (mb)

Isotope	Ma 67	Ko 78	Mi 79	this work
^{148}Sm	257 $\pm$ 50	281 $\pm$ 23		269 $\pm$ 12
^{149}Sm	1620 $\pm$ 280		2490 $\pm$ 200	1489 $\pm$ 65
^{150}Sm	370 $\pm$ 72	690 $\pm$ 51		458 $\pm$ 18

Ma 67 R.L. Macklin, J.H. Gibbons, Phys. Rev. 159 (1967) 1007

Ko 78 V.N. Kononov et al., Sov. J. Nucl. Phys., 27 (1978) 5

Mi 79 M. Mizumoto et al., Proc. Int. Conf. on Nucl. Cross Sections for Technology, Knoxville, Tennessee, p. 328 (1979)

Comparison of the results in Table I shows that good agreement is found only for ^{148}Sm. For the other two isotopes severe discrepancies could be resolved by the present measurement.

For the (astrophysically important) cross section ratio $\sigma^{148}Sm/\sigma^{150}Sm$ part of the quoted uncertainty cancels out yielding

$$\frac{(\sigma N)^{148}Sm}{(\sigma N)^{150}Sm} = 0.90 \pm 0.03.$$

This value being significantly different from unity implies a branching of the s-process capture path at ^{147}Nd and $^{147,148}Pm$. In order to analyse these branchings, the capture cross sections of the unstable branching isotopes were calculated according to the Hauser-Feshbach formalism using a consistent set of carefully evaluated parameters. These cross sections are summarized in Table II.

Table II Calculated capture cross sections for the unstable isotopes ^{147}Nd, ^{147}Pm, ^{148}Pm and ^{151}Sm (mb).

Neutron energy (keV)	Capture cross section (mb)* ^{147}Nd	^{147}Pm	^{148}Pm	^{151}Sm
1	7940	14500	19100	22000
10	1240	2260	3060	3880
20	794	1413	1897	2463
30	629	1110	1489	1953
50	482	849	1147	1501
100	264	588	736	805
$\frac{<\sigma v>}{v_T}$ (kT=30keV)	625	1163	1542	1932

* estimated uncertainty ± 30 %

With all this informations constraints for the shape and the normalization of the $\sigma N(A)$-curve as well as for the neutron density during the s-process were derived.

+ Denison University, Granville, Ohio 43023, USA

++ E.N.E.A., Via Mazziniz, I-43100 Bologna, Italy

1.11 ^{178,179,180}Hf and ^{180}Ta(n,γ) Cross Sections and their Contribution to Stellar Nucleosynthesis*

H. Beer and R. L. Macklin[+]

The neutron capture cross sections of ^{178,179,180}Hf were measured in the energy range 2.6 keV to 2 MeV. The average capture cross sections were calculated and fitted in terms of strength functions. Resonance parameters for the observed resonances below 10 keV were determined by a shape analysis. Maxwellian averaged capture cross sections were computed for thermal energies kT between 5 and 100 keV. The cross sections for kT = 30 keV were used to determine the population probability of the 8^- isomeric level in ^{180}Hf by neutron capture as (1.24 $\pm$ 0.06) % and the r-process abundance of ^{180}Hf as 0.0290 (Si $\equiv 10^6$). These quantities served to analyze s- and r-process nucleosynthesis of ^{180}Ta.

---

* Phys. Rev. C 26, 1404 (1982)

\+ Oak Ridge National Laboratory, Oak Ridge, Tennessee 37830, USA

1.12 The Solar Mercury Abundance*

G. Walter, H. Beer

The neutron capture cross sections of the reactions ^{198}Hg(n,γ)^{199}Hg^m and ^{202}Hg(n,γ)^{203}Hg have been measured by the activation method at 25 keV. The cross section of ^{202}Hg allowed an estimate of the solar mercury abundance $N_\odot$(Hg) via s-process systematics. $N_\odot$(Hg) was found to be 0.21 / 10^6Si.

---

* accepted for publ. in Astronomy and Astophysics

1.13 Neutron Capture and Fission Cross Section of ^{243}Am in the Energy Range from 5 to 250 keV*

K. Wisshak and F. Käppeler

(Relevant to request numbers 721101, 732104, 741128, 761100, 762028, 792147, 792237, 794005, 812047, 712111, 792146, 792236)

The neutron capture and subthreshold fission cross section of ^{243}Am was measured in the energy range from 5 to 250 keV using ^{197}Au and ^{235}U as the respective standards. Neutrons were produced via the ^{7}Li(p,n) and the T(p,n) reaction with the Karlsruhe 3-MV pulsed Van de Graaff accelerator. Capture events were detected by two Moxon-Rae detectors with graphite and bismuth graphite converters, respectively. Fission events were registered by a NE-213 liquid scintillator with pulse-shape discriminator equipment. Flight paths as short as 50 - 70 mm were used to obtain an optimum signal-to-background ratio. After correction for the different efficiency of the individual converter materials the capture cross section could be determined with a total uncertainty of 3 - 6 %. The respective values for the fission cross section are 8 - 12 %. The results are compared to predictions of recent evaluations, which in some cases are severely discrepant.

---

* KfK-Report 3503 and submitted for publ. to Nucl. Sci. Eng.

KERNFORSCHUNGSZENTRUM KARLSRUHE
INSTITUT FÜR KERNPHYSIK

1. Neutron and Charged-Particle Yields and Spectra from 590 MeV Proton Bombardment of Thick Uranium Targets

F. Raupp, S. Cierjacks, Y. Hino, S.D. Howe [1], M.T. Rainbow [2], M.T. Swinhoe [3] and L. Buth [4]

The analysis of experimental data measured previously at the SIN cyclotron [1] has been completed. The final publication of these data [2] contains absolute neutron yields for several penetration depths of protons into a 10×10 cm^2, 40 cm long, uranium block. Differential yields are given for three laboratory angles of 30^o, 90^o and 150^o, and for five average penetration depths of 2.5, 7.5, 12.5, 17.5, and 22.5 cm of primary protons. The differential spectra cover the secondary neutron energy range from 0.7 to 590 MeV. Integration of these data over the entire target length and all emission angles provided a total neutron yield of 24.3 ± 4 n/p in accordance with previous results for this quantity [3]. In addition to neutron yields, charged particle production yields for secondary protons, deuterons, tritons and pions ($\pi^+ + \pi^-$) have also been determined for the same range of emission angles and penetration depths into target. A typical example of results obtained from this work is shown in Fig. 1. This figure exhibits the differential production yields of protons and deuterons emitted from the target block at a laboratory angle of 90^o. The yields of protons and deuterons with energies higher than ~ 50 MeV are of about the same size for the two primary proton penetration depths of 2.5 and 7.5 cm. But, the yields of secondary deuterons are more than one order of magnitude smaller than those of secondary protons.

2. Systematics of Angular-Dependent Neutron Production by 590 MeV Protons on Thin Targets with $12 \leq A \leq 238$.

S. Cierjacks, Y. Hino, F. Raupp, S.D. Howe [1] and L. Buth [4]

In continuation of our previous studies on neutron production in thin metal targets [4] additional measurements have been performed at the SIN cyclotron employing a

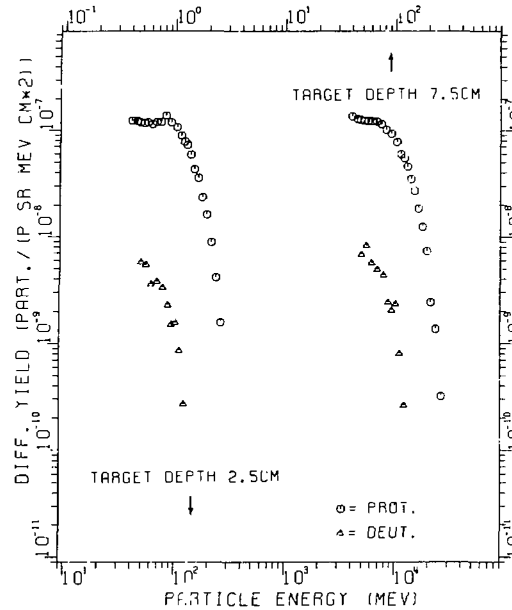

Fig. 1 Differential yields of secondary protons and deuterons emitted from a thick uranium target at a laboratory angle of 90°. The two sets of of curves refer to 2.5 and 7.5 cm average depths of 590 MeV primary protons into target.

new "open geometry" setup which allowed to extend the previously studied angular range. The new measurements provided experimental data for seven elements between carbon and lead at laboratory angles of 23° and 90°. As previously, neutron spectrum data were taken in the energy range 0.8 to 590 MeV. The analyses of all experimental data taken in 1981 and 1982 have been finalized, and preliminary data were presented at the 1982 Antwerp Conference [5]. The differential neutron production cross sections for eight target nuclei at a laboratory angle of 30° are shown in Fig. 2. All individual curves exhibit the well-known two-component shape resulting from evaporation and cascade processes, respectively. The cross sections increase smoothly with increasing mass of the target nucleus, and the fraction of cascade neutrons ($E_n \gtrsim 15$ MeV) tends to increase with decreasing target mass number. The experimentally determined neutron production cross sections are presently used for extensive tests of model predictions provided by the High Energy Nucleon-Meson Transport Code (HETC) [6] (see also Section 4).

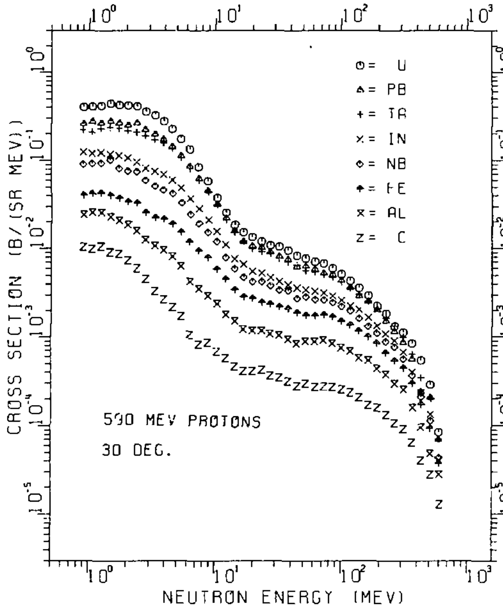

Fig. 2 Differential cross sections for neutrons produced by 590 MeV proton bombardment of thin metal targets. Data are given for a laboratory angle of 30°.

3. Systematics of Angular-Dependent Charged-Particle Production by 590 MeV Protons on Thin Targets with $12 \leq A \leq 238$

S. Cierjacks, S.D. Howe [1], Y. Hino, F. Raupp, and L. Buth [4]

The previously described experiments on charged particle production by 590 MeV protons [7] have been continued. Supplementary measurements on thin targets of C, Al, Fe, Nb, In, Ta and lead at laboratory angles of 23° and 90° were performed in 1982. The evaluation of the experimental data for eight targets and five emission angles is in a final stage and completion is expected by the end of 1983. The final results are expected to provide differential production cross sections for secondary protons, deuterons, tritons, and pions ($\pi^+ + \pi^-$) at emission angles of 23°, 45°, 90°, 135°, and 157° and thin targets of C, Al, Fe, Nb, In, Ta, Pb, and U. These data are considered to give an additional important piece of information for comparisions with present HETC model predictions. Preliminary cross sections for the production of deuterons and tritons are shown in Figs. 3 and 4. In a semilogarithmic plot of production cross sections as a function of particle energy the data follow almost a straight line with slopes

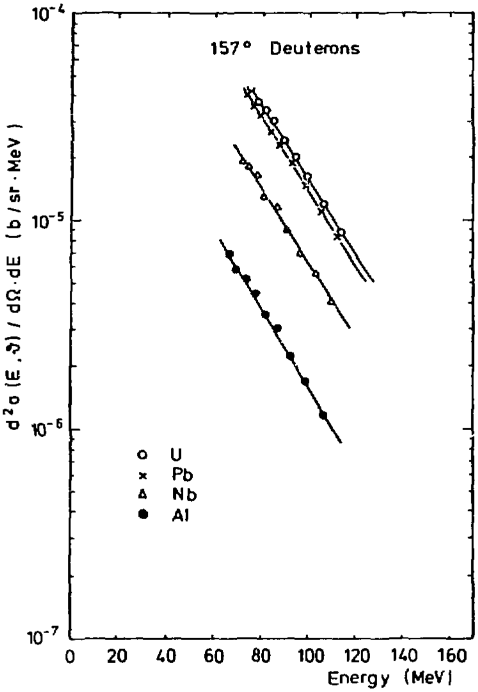

Fig. 3
Differential cross sections for secondary deuterons produced by 590 MeV protons on thin uranium, lead, niobium and aluminum targets. Preliminary values are given for a laboratory angle of 157°.

Fig. 4
Differential cross sections for secondary tritons produced by 590 MeV protons on thin uranium, lead, niobium and aluminum targets. The preliminary data refer to a laboratory angle of 90°.

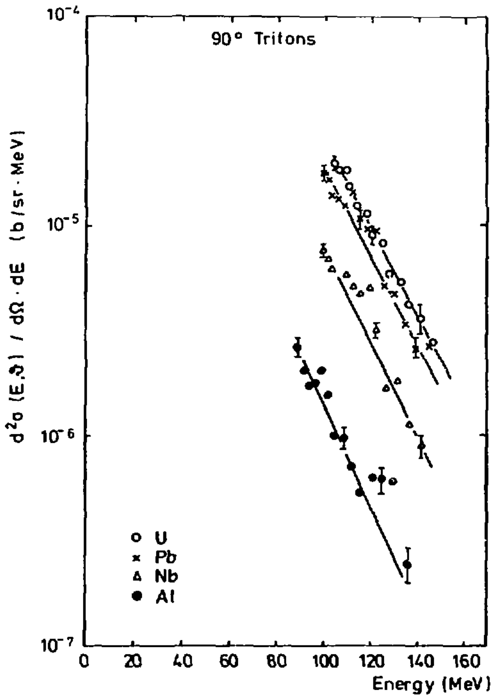

increasing slightly with increasing emission angle. The high absolute cross sections above ~ 50 MeV and their particular energy dependences are possibly indicative of a nucleon clustering in the target during the cascade process.

4. Intercomparisons of Measured and Calculated Neutron and Charged Particle Production Cross Sections

S. Cierjacks, Y. Hino, T.W. Armstrong [5], and D. Filges [5].

Systematic tests of the accuracy of model predictions from HETC calculations are presently being performed within the frame-work of a KfK-KFA collaboration. During the period covered in this report work has concentrated on neutron production cross sections [5,8]. Comparisons of measured and calculated data revealed that the neutron production cross sections in the evaporation range ($E_n \lesssim 15$ MeV) can sufficiently be predicted by the HETC-Code for emission angles of 30^o, 90^o, and 150^o. For the cascade region, however, large discrepancies continue to persist, and the discrepancies increase rapidly with increasing neutron energy and emission angle. A recent comparison of measured and calculated cross sections is shown in Fig. 5. The results given for a thin Ta - target and a laboratory angle of 150^o demonstrate that the calculated cross sections above $E_n \gtrsim 100$ MeV are already bv almost an order of magnitude smaller than the measured ones.

5. Surveys on Instrumental Developments

S. Cierjacks

In addition to the experimental work on neutron and charged-particle production by high-energy protons, some reviews on the present instrumental situation in nuclear data research have been provided. A survey on instrumental developments in high-resolution neutron measurements has been prepared and presented at the Europhysics Topical Conference on Neutron Induced Reactions [9]. For inclusion in the second volume of the NEANDC (OECD) Series on Neutron Physics and Nuclear Data in Science and Technology a review on accelerator-based pulsed white neutron sources has been provided and published [10]. Finally, a seminar on high- energy, high-intensity neutron sources has been prepared for presentation at the Service de Physique Neutronique et Nucléaires of the Centre de Bruyères-le Châtel [11].

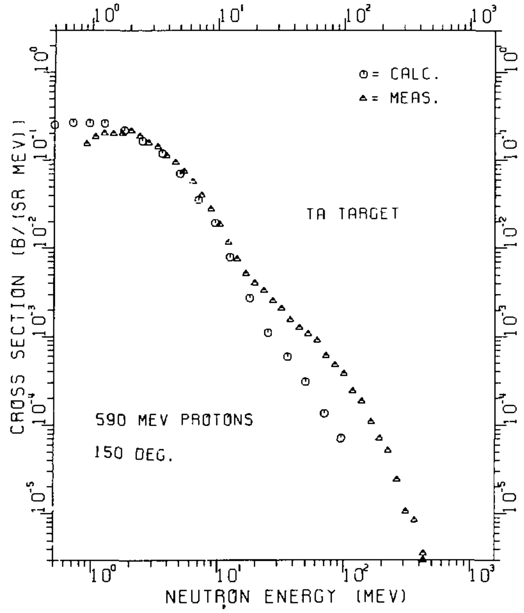

Fig. 5 Comparison of measured and calculated differential cross sections for neutron production by 590 MeV protons at a laboratory angle of 150°. It can be seen that HETC-model calculations provide reasonable predictions in the neutron evaporation range ($E_n \lesssim 15$ MeV), but underestimate the data increasingly in the cascade region ($15 \lesssim E_n \lesssim 100$ MeV).

---

[1] Now at Los Alamos National Laboratory, Los Alamos, New Mexico 87545, U.S.A.

[2] Now at AAEC Research Establishment, Lucas Heights, Sutherland 2232, N.S.W., Australia

[3] Now at AERE Harwell, Didcot, Oxfordshire, OX11 ORA, U.K.

[4] Permanent member of the Institut für Neutronenphysik und Reaktortechnik, Kernforschungszentrum Karlsruhe

[5] Institut für Reaktorentwicklung, Kernforschungsanlage Jülich, Postfach 1913, D-5170 Jülich 1

References

[1] S. Cierjacks, M.T. Rainbow, M.T. Swinhoe and L. Buth, Neutron and Charged Particle Production Yields and Spectra from Thick Targets by 590 MeV Protons, KfK-3097B, Kernforschungszentrum Karlsruhe, Dec. 1980

[2] F. Raupp, Messung der orts- und winkelabhängigen Spektren schneller Neutronen und geladener Sekundärteilchen aus Spallationsreaktionen von 590 MeV Protonen in dicken Urantargets, KfK-3511B, Kernforschungszentrum Karlsruhe, 1983

[3] J.S. Fraser, R.E. Green, J.W. Hilborn, J.C.D. Milton, W.A. Gibson, E.E. Gross and A. Zucker, Phys. in Can. 21, 17 (1965)

[4] S. Cierjacks, Y. Hino, S.D. Howe, F. Raupp, L. Buth, M.T. Rainbow and M.T. Swinhoe, Measurements of Differential Production Cross Sections for Neutrons by 590 MeV Protons, Progr. Rep. on Nuclear Data Research in the Federal Republic of Germany for the Period April 1, 1981 to March 31, 1982; NEANDC (E) - 232 U Vol. V, INDC (Ger)-24/L+S, FIZ-KA--4, 1982, p. 8

[5] S. Cierjacks, Y. Hino, S.D. Howe, F. Raupp and L. Buth, Differential Neutron Production Cross Sections for 590 MeV Protons, Proc. Conf. on Nuclear Data for Science and Technology, Antwerp, Sept. 1982 (D. Reidel Publishing Comp., Dordrecht, 1983), p. 383

[6] HETC-ORNL-4744, Oak Ridge National Laboratory, 1972

[7] S.D. Howe, S. Cierjacks, Y. Hino, F. Raupp, M.T. Rainbow, M.T. Swinhoe and L. Buth, Differential Cross Sections for Charged Particles Produced by 590 MeV Proton Bombardment of Thin Metal Targets, ICANS-V, Proc. 5th Meeting of the Int. Coll. on Advanced Neutron Sources, G.S. Bauer and D. Filges (Eds.), Jül-Conf-45, 1981, p. 313

[8] T.W. Armstrong and D. Filges, Model Predictions of Differential Neutron Production Cross Sections for Lead and Uranium Bombarded by 590 MeV Protons, Proc. Conf. on Nuclear Data for Science and Technology, Antwerp, Sept. 1982, (D. Reidel Publishing Comp., Dordrecht, 1983), p. 387

[9] S. Cierjacks, Instrumental Developments in High Resolution Neutron Measurements, Proc. Europhysics Conf. on Neutron Induced Reactions, Smolinice, CS, June 1982 (Slovac Academy of Sciences, Bratislava, 1982) p. 423; and KfK-3447B, Kernforschungszentrum Karlsruhe, June 1982

[10] S. Cierjacks, Accelerator-based Pulsed White Neutron Sources, in "Neutron Sources for Basic Physics and Applications" (Neutron Physics and Nuclear Data in Science and Technology, Vol. 2); S. Cierjacks (Ed.), Pergamon Press, Dec 1982, p. 81-132

[11] S. Cierjacks, High-energy, High-intensity Neutron Sources, Seminar presented at the Service de Physique Neutronique et Nucléaire, C.E. de Bruyères-le-Châtel, France, Dec. 1982

KERNFORSCHUNGSZENTRUM KARLSRUHE
INSTITUT FÜR NEUTRONENPHYSIK UND REAKTORTECHNIK

1. Nuclear Data Evaluation

1.1 Reevaluation of ^{243}Am Subthreshold Fission Cross Section

F.H. Fröhner, B. Goel and B. Krieg

(Relevant to request numbers 712111, 712114, 792146, 792236)

Our recent evaluation of ^{243}Am neutron cross sections for the KEDAK file [1] was handicapped by a complete lack of reliably measured fission cross section data in the subthreshold region below 250 keV. Therefore the Hauser-Feshbach formalism with Hill-Wheeler barrier penetrabilities was employed to extrapolate the data of ref. [2] from 250 keV downwards. The resulting curve was very close to the JENDL-2 curve shown in Fig. 1. Recent measurements performed at Karlsruhe [3] between 10 and 250 keV showed, however, that the extrapolation was about 40 % low. The new data could be fitted with modified fission barrier parameters. The fit, labeled KEDAK-4, is shown in Fig. 1 together with other recent evaluations [4-6] and the experimental data. As in the case of ^{241}Am the bomb-shot data of Seeger et al. [7], on which the ENDF/B-V curve is based, must be considered as unreliable.

References

[1] F.H. Fröhner, B. Goel, U. Fischer and H. Jahn, Proc. Conf. on Nucl. Data for Science and Technology, Antwerp 1982, Dordrecht etc. (1983), p. 211

[2] J.W. Behrens and J.C. Browne, Nucl. Sci. Eng. 77(1980)148

[3] K. Wisshak and F. Käppeler, Report KfK 3503, Karlsruhe (1983), submitted for publication in Nucl. Sci. Eng.

[4] R. Kinsey (compil.), Report ENDF-201,Brookhaven (1979)

[5] Y. Kikuchi, Report JAERI-M 83-096, JAERI (1982)

[6] M. Sowerby, private communication

[7] P.A. Seeger, A. Hemmendinger and B.C. Diven, Nucl. Phys. A96(1967)605

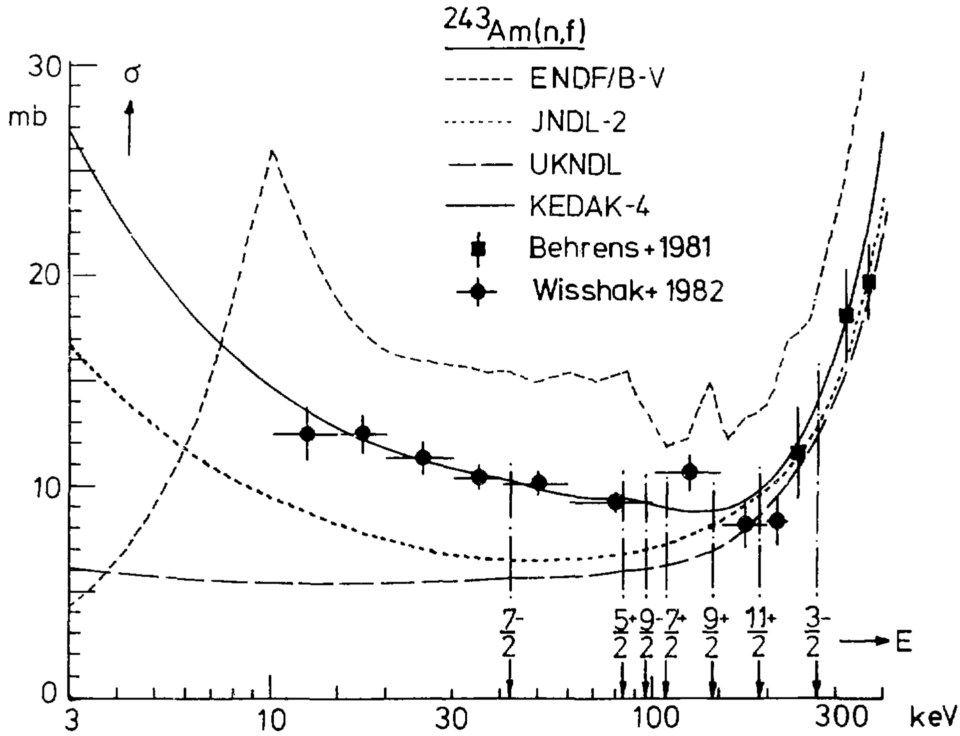

Fig. 1 - New KEDAK-4 evaluation of the ^{243}Am fission cross section between 3 and 400 keV shown together with experimental data [2, 3] and other recent evaluations [4-6]. Inelastic thresholds are indicated by arrows and spin-parity characteristics of residual levels.

1.2 Statistical Inference of Level Densities from Resolved Resonance Parameters

F.H. Fröhner

Methods for estimation of level densities from resonance parameters (level energies, entrance channel widths, level spins and parities) have been reviewed [1]. The main conclusions were as follows.

- Ladder statistics, even those based on random matrix theory such as the Δ_3 and W statistics of Dyson and Mehta, are unreliable because of low sensitivity to missing and spurious levels.

- The number of missing levels is best estimated from a comparison of the observed entrance-channel width distribution with the expected Porter-Thomas distribution. Maximum-likelihood estimation is the appropriate approach. In simple situations it yields rigorous (Bayesian) solutions, in more complicated cases nearly rigorous solutions, including error estimates. Analytical extensions to mixed sequences and unresolved multiplets are available.

For the practically important case of a Porter-Thomas distribution, truncated below a sharp detection threshold whose height is unknown but whose energy dependence can be inferred from the cumulative level number staircase plot, the following Bayesian solution was newly derived,

$$\frac{1}{N-1}\sum_{i=1}^{N}\Gamma_i = \langle\Gamma\rangle\left(1+\frac{2}{\sqrt{\pi}}\frac{e^{-x_1}\sqrt{x_1}}{\operatorname{erfc}\sqrt{x_1}}\right) \qquad \text{with} \qquad x_1 \equiv \frac{\Gamma_1}{2\langle\Gamma\rangle} ,$$

$$\bar{u}_c = \frac{N+1}{N}\,\frac{\operatorname{erfc}\sqrt{x_1}}{f(E_1)} .$$

Here Γ_i ($i = 1, 2, \ldots, N$) are the observed reduced widths, Γ_1 the one which is relatively closest to the threshold, $\langle\Gamma\rangle$ the ensemble average, $\bar{u}_c$ the average observed fraction of levels, and $f(E)$ its energy dependence, $u_c(E) = \bar{u}_c f(E)$. The two quantities to be estimated are $\langle\Gamma\rangle$ and $\bar{u}_c$. $\langle\Gamma\rangle$ is obtained from the first equation, $\bar{u}_c$ follows then from the last one. For mixed level sequences one finds similar, but more complicated systems of equations which can no longer be solved independently (see [1].

Reference

[1] F.H. Fröhner, Report KfK 3553, Karlsruhe (1983); Proc. Meeting on Basic and Applied Problems of Nuclear Level Densities, Brookhaven, 11-15 April 1983 (in print); for a less complete version see Proc. Conf. on Nucl. Data for Sci. and Technol., Antwerp 1982, Dordrecht (1983), p. 623

INSTITUT FÜR CHEMIE (1): NUKLEARCHEMIE
KERNFORSCHUNGSANLAGE JÜLICH

1. Neutron Data

1.1 Study of (n,t) and (n,^{3}He) Reactions

S.M. Qaim, G. Stöcklin, S. Sudar, R. Wölfle

Radiochemical studies on fast-neutron induced trinucleon emission reactions were continued. We recently reported excitation functions of (n,t) reactions on ^{27}Al, ^{59}Co and ^{93}Nb up to incident neutron energies of 20 MeV [1]. Since monoenergetic neutrons of energies > 20 MeV are rarely available, we thought it worthwhile to determine an (n,t) excitation function using d(Be) breakup neutron spectra. At first the neutron spectra produced via breakup of deuterons of energies 17.5, 20.0, 22.5, 25.0, 27.5 and 30.0 MeV were characterized by the multiple foil activation technique using various threshold reactions. Spectrum unfolding was done using SAND II and RFSP codes. Thereafter aluminium sheets were irradiated with various neutron spectra. Tritium was separated from each sample by vacuum extraction and counted in the gas phase using a low-level β^- detector. Using the same iterative calculational methods as for the spectrum unfolding it was possible to construct the excitation function of the ^{27}Al(n,t)^{25}Mg reaction. Refinements in the calculational method are underway to be able to apply it to other target nuclei.

The (n,^{3}He) reactions on nuclei with A > 120 were investigated both radiochemically and mass spectrometrically. The ^{3}He/^{4}He emission cross-section ratios are shown in Fig. 1 as a function of increasing Z of the target element. The activation and mass spectrometric data agree within about 30%. The ratio increases up to Z $\sim$ 44 beyond which the trend is reversed. Presumably the increase in the ratio for elements with Z $\leq$ 44 is due to a sharper decrease in the (n,α) cross section with increasing Z as compared to that in the case of the (n,^{3}He) cross section. In the heavier elements (Z > 44), on the other hand, the ratio decreases possibly due to the sharper decrease in the latter cross section.

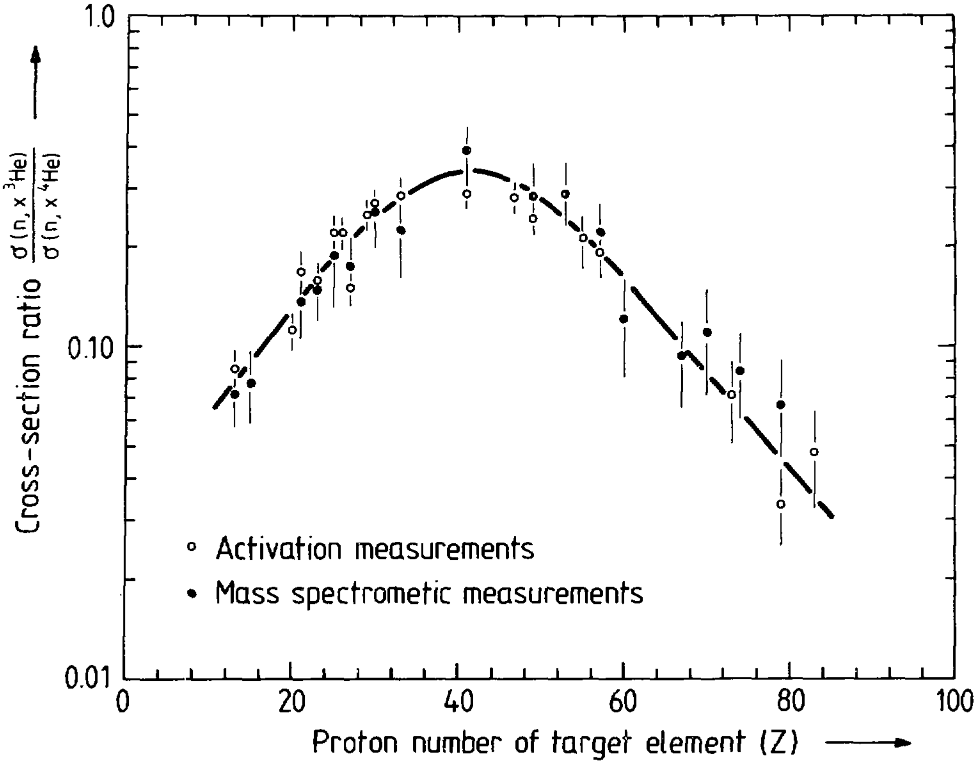

Fig. 1 ^{3}He to ^{4}He emission cross-section ratio as a function of Z of the target element. The activation data describe the ratio of $\sigma(n,{}^{3}He + dp + n2p)$ to $\sigma(n,{}^{4}He + 2n2p)$; the mass spectrometric data give $\sigma(n,x{}^{3}He)/\sigma(n,x{}^{4}He)$.

The present state of knowledge on complex particle emission in fast neutron induced reactions was reviewed [2].

1.2 Cross Section Measurements of Hydrogen and Helium Producing Reactions induced by 4 to 9 MeV Neutrons

S.M. Qaim, G. Stöcklin, R. Wölfle

(Relevant to request identification numbers: 752244 F, 762107 F, 762108 F, 762242 F, 792209 R, 792210 R, 801147 R)

In continuation of our cross-section measurements for ^{58}Ni in the energy range of 4 to 9 MeV, described in last year's report, we now determined the excitation functions for the reactions $^{58}Ni(n,\alpha)^{55}Fe$, $^{62}Ni(n,\alpha)^{59}Fe$, $^{61}Ni(n,p)^{61}Co$ and $^{62}Ni(n,p)^{62}Co$. All the measurements have been done for the first time. Some of the results were presented at the Antwerp conference [3].

Measurements on (n,n'p) reactions, similar to those at 14 MeV [cf. 4], are in progress.

1.3 Measurement of $^{7}Li(n,n't)^{4}He$ Reaction Cross Sections

H. Liskien*, S.M. Qaim, R. Wölfle

(Relevant to request identification numbers: 722069 F, 724007 F, 724008 F, 732004 F, 762246 F, 781159 F, 792105 F)

Cross-section measurements using separation and gas phase counting of tritium over the energy range of 13 to 16 MeV were completed. The results have uncertainties of 6 to 7% over the entire energy range covered, i.e. from threshold to 16 MeV. They are higher than recent Harwell results but about 15% lower than the ENDF B-IV results. The data were presented at the Antwerp conference [5].

*CBNM, Geel, Belgium

2. Charged Particle Data for Radioisotope Production

H. Döhler, S.M. Qaim, G. Stöcklin, J.H. Zaidi

In continuation of our studies [6-9] on the production of medically important short-lived radioisotopes, cross-section measurements were performed on some nuclear reactions relevant to the production of ^{123}I and ^{117m}Sn.

Studies on the $^{122}Te(d,n)^{123}I$ reaction were completed. Measurements were also performed on deuteron induced reactions on natural tellurium.
A comparison of the three direct methods used for the production of ^{123}I,

namely $^{124}Te(p,2n)^{123}I$, $^{123}Te(p,n)^{123}I$ and $^{122}Te(d,n)^{123}I$, shows that the (d,n) reaction gives the least contamination from ^{124}I; the thick target yield, however, is rather low [10].

^{117m}Sn($T_{1/2}$ = 13.6 d) is a potentially important radioisotope. It emits almost a single photon of 159 KeV energy which is ideally suited for single photon emission computed tomography (SPECT). Due to its high spin ($11/2^-$) it can, however, be produced only via a high energy reaction. We investigated the following four reactions for its possible production: $^{nat}Cd(\alpha,xn)^{117m}Sn$, $^{nat}Cd(^3He,xn)^{117m}Sn$, $^{nat}In(\alpha,pxn)^{117m}Sn$ and $^{nat}In(^3He,pxn)^{117m}Sn$. The $^{nat}In(\alpha,pxn)^{117m}Sn$ reaction was found to be the most suitable. Cross sections for this reaction were then measured up to 140 MeV. The thick target yield over the optimum energy range of 45 $\rightarrow$ 20 MeV was found to be 9 μCi/μAh.

In addition to the experimental work on excitation functions, a survey of nuclear data relevant to medically important radioisotopes was carried out [11] and a group report on the data relevant to the cyclotron production of some short-lived radiohalogens was prepared and presented at the Antwerp conference [12].

References

[1] S.M. Qaim, R. Wölfle, H. Liskien, Excitation functions of (n,t) reactions on ^{27}Al, ^{59}Co and ^{93}Nb, Phys. Rev. C25 (1982) 203

[2] S.M. Qaim, Complex particle emission in fast neutron induced reactions, Proc. Europhysics Topical Conference on Neutron Induced Reactions, Smolenice, June 1982 (Slovak Academy of Sciences, Bratislava, 1982) p. 291

[3] S.M. Qaim, R. Wölfle, G. Stöcklin, Cross sections for hydrogen and helium producing reactions induced by fast neutrons on potential first wall materials of fusion reactor technology, Proc. Conf. on Nuclear Data for Science and Technology, Antwerp, September 1982 (D. Reidel Publishing Company, Dordrecht, 1983) p. 356

[4] S.M. Qaim, A systematic study of (n,d), (n,n'p) and (n,pn) reactions at 14.7 MeV, Nucl. Phys. A382 (1982) 255

[5] H. Liskien, R. Wölfle, S.M. Qaim, Determination of $^{7}Li(n,n't)^{4}He$ cross sections, Proc. Conf. on Nuclear Data for Science and Technology, Antwerp, September 1982 (D. Reidel Publishing Company Dordrecht, 1983) p. 349

[6] He Youfeng, S.M. Qaim, G. Stöcklin, Excitation functions for ^{3}He-particle induced nuclear reactions on ^{76}Se, ^{77}Se and ^{nat}Se: Possibilities of production of ^{77}Kr, Int. J. appl. Radiat. Isotopes 33 (1982) 13

[7] Z.B. Alfassi, R. Weinreich, The production of positron emitters ^{75}Br and ^{76}Br: Excitation functions and yields for ^{3}He- and α-particle induced nuclear reactions on arsenic, Radiochimica Acta 30 (1982) 67

[8] S.M. Qaim, H. Ollig, G. Blessing, A comparative investigation of nuclear reactions leading to the formation of short-lived ^{30}P and optimization of its production via the $^{27}Al(\alpha,n)^{30}P$ process at a compact cyclotron, Int. J. appl. Radiat. Isotopes 33 (1982) 271

[9] R. Weinreich, J. Knieper, Production of ^{77}Kr and ^{79}Kr for medical applications via the proton irradiation of bromine: Excitation functions, yields and separation procedure, Int. J. appl. Radiat. Isotopes, in press

[10] J.H. Zaidi, S.M. Qaim, G. Stöcklin, Excitation functions of deuteron induced nuclear reactions on natural tellurium and enriched ^{122}Te: Production of ^{123}I via the $^{122}Te(d,n)^{123}I$-process, Int. J. appl. Radiat. Isotopes, in press

[11] S.M. Qaim, Nuclear data relevant to cyclotron produced short-lived medical radioisotopes, Radiochimica Acta 30 (1982) 147

[12] S.M. Qaim, G. Stöcklin, R. Weinreich, H. Backhausen, Z.B. Alfassi, J.H. Zaidi, Recent nuclear data measurements relevant to the cyclotron production of some medically important short-lived radiohalogens, Proc. Conf. on Nuclear Data for Science and Technology, Antwerp, September 1982 (D. Reidel Publishing Company, Dordrecht, 1983) p. 909

I. INSTITUT FÜR EXPERIMENTALPHYSIK
UNIVERSITÄT HAMBURG

1. Spin Depletion by Preequilibrium Neutron Emission in ^{3}He Induced Reactions

A. Schüring, W. Scobel

Preequilibrium emission (PE) influences the energy and spin population of the residual nuclei. If they are radioactive and have a spin isomer, the excitation functions $\sigma_{gs}(E)$ and $\sigma_{ms}(E)$ for the population of ground and isomeric state, respectively may be measured with activation techniques; the isomeric cross section ratio σ_{gs}/σ_{ms} then provides an integral measure of the spin distribution in the residual, particle stable nucleus.

We have measured the ^{109}Ag(^{3}He,xn)$^{112-x}$In reactions for x = 1-5 and projectile energies $E \leq 43$ MeV. Single foils and foil stacks including aluminium degraders have been irradiated and then analyzed with a Ge(Li) detector. The reactions and their spectroscopic data are listed in Table I. The excitation functions obtained are shown in Fig. 1 together with model calculations.

It can be seen that the Ewing-Weisskopf model cannot explain the high energy tails of the excitation functions; combining this model, however, with a preceding PE step considerably improves the agreement. We have applied the revised hybrid model [1] with an initial configuration of $n_0 = 4$ excitons (1.5 neutrons, 2.5 protons, no hole and a mean free path multiplier k=1.5).

Calculations of the isomeric ratio in the framework of the pure Hauser-Feshbach model, including γ-deexcitation with multipolarities $L \leq 3$, indicate too strong a population of the ground (i.e. high spin) state whenever PE dominates in the excitation functions. If we assume [2] that (i) the PE depletion as given by the hybrid model is equally distributed over all partial waves of the entrance channel and (ii) the angular momentum carried away by the PE neutron, due to its forward peaked angular distribution, is parallel to that of the reaction system ^{112}In*, we obtain a spin population (see Fig. 1) that results in a calculated isomeric ratio that is much closer to the experimental values, in particular, if the spin cut off parameter σ is reduced to 70% of the rigid body value σ_{rig}.

Table I. Reactions and γ-spectroscopic data of the residual nuclei (target spin is $9/2^+$).

Reaction	State	I^π	$T_{1/2}$	E_γ (keV)	Branching ratio
$^{109}Ag(^3He,n)^{111}In \rightarrow {}^{111}Cd$	gs	$9/2^+$	2,83 d	171,3 245,4	99,99 100
	ms	$1/2^-$	7,7 m	536,9	100
$^{109}Ag(^3He,2n)^{110}In \rightarrow {}^{110}Cd$	gs	7^+	4,9 h	884,7 937,5	91,98 69,57
	ms	2^+	69 m	657,7	99,07
$^{109}Ag(^3He,3n)^{109}In \rightarrow {}^{109}Cd$	gs	$9/2^+$	4,3 h	203,3 623,8 1148,8	74,0 5,3 5,2
	ms	$1/2^-$	1,3 m	650,0	100
$^{109}Ag(^3He,4n)^{108}In \rightarrow {}^{108}Cd$	gs	6^+	58 m	242,8 326,0 569,0 730,8 875,5 1033,0 1056,9	38,28 12,84 5,0 8,24 89,0 24,9 31,44
	ms	3^+	40 m	968,5 1529,4	4,35 7,264
$^{109}Ag(^3He,5n)^{107}In \rightarrow {}^{107}Cd$	gs	$9/2^+$	32,4 m	204,95 320,94	32,4 10,2

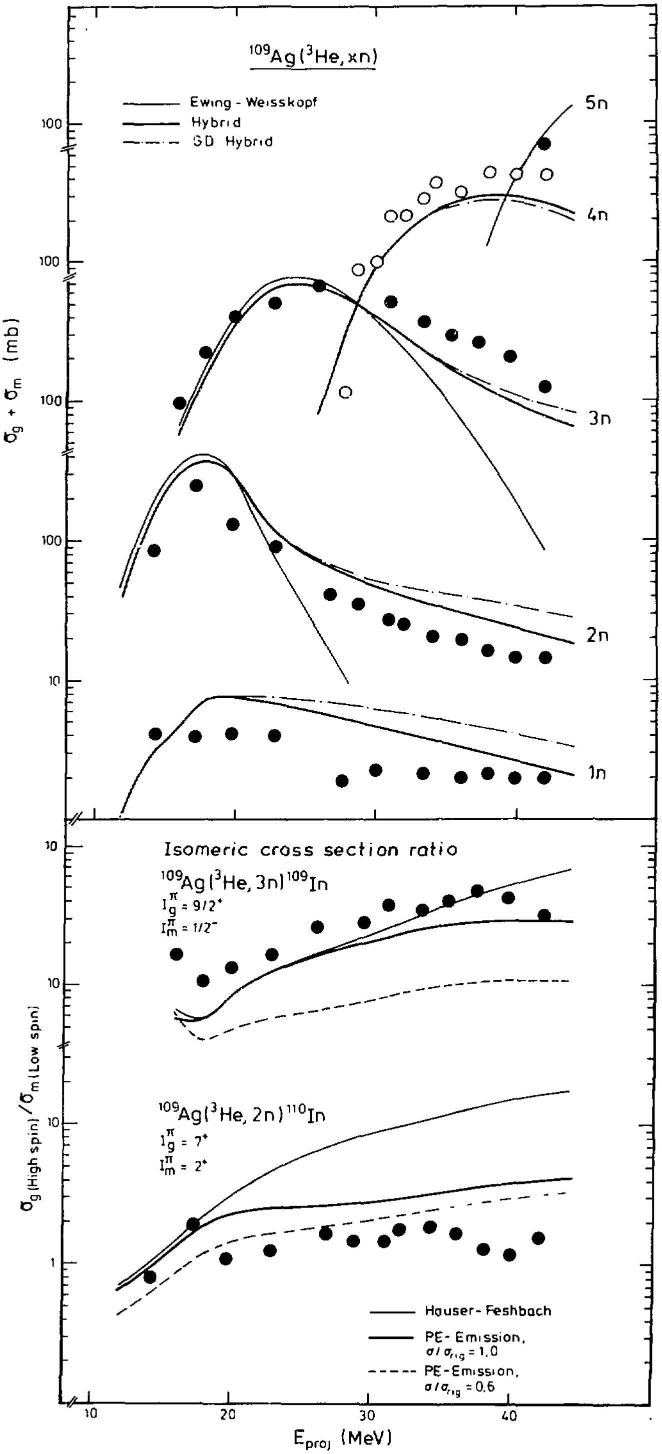

Fig. 1 Excitation functions and isomeric ratios for $^{109}Ag(^3He,xn)$. Calculations are performed without and with preequilibrium competition and for different values of the spin cut off parameter σ in terms of the rigid body value σ_{rig}.

References

[1] M. Blann, H. Vonach, Report UCRL 88540 (1982); M. Blann, J.Bisplinghoff, Code ALICE/LIVERMORE 82, Report UCID-19614 (1982)

[2] H.H. Bissem, W. Scobel, Nukleonika 26(1981), in press

INSTITUT FÜR REINE UND ANGEWANDTE KERNPHYSIK

UNIVERSITÄT KIEL, FORSCHUNGSREAKTOR GEESTHACHT

Fast-Chopper Time-of-Flight Spectrometer

H.-G. Priesmeyer, B. Asmussen, P. Fischer, U. Harz, P. Henkens

1.) Improvements concerning the Experiment (U. Harz)

An HP-1000 system has been installed for data collection, control of the experiment and the analysis of data (transmission, shape and area analysis).
A new time-of-flight device has been developed with a derandomizing capacity of 128 events.

2.) Total Cross Section of Bound Proton in Zirconiumhydride at 4.7K (P.Fischer)

The systematic investigations of the proton harmonic oscillator levels as a function of temperature have been completed by a measurement at 4.7K.

In figure 1 the spectrum at 4.7K is shown. The first minimum has the form of a sharp cusp, but the cross section of the free proton is not reached.

3.) Construction of a 24 keV-Ironfilter (P. Henkens, H.-G. Priesmeyer)

A portable iron filter - consisting of 35 cm of 99.85 %ARMCO iron, 23 cm of aluminium and 7.5 cm of sulfur - has been designed to be used for cross section measurements, neutronradiography and/or hydrogen content determinations in ferrous materials.
Figure 2 is a fast-chopper transmission measurement from > 300 to 3.5 keV showing the 24 keV line and additional high-energy contamination around 300 keV (presumably enhanced by the use of Li-6 glass detectors). They can be suppressed by a filter difference measurement using 5 mm of Ti, which reduces the 24 keV signal by about 30 %.

+ work supported by GKSS under contract 251897

4.) Monte-Carlo calculations for a Neutron Guide Tube (H.G.Priesmeyer)

Computational investigations have been made on a neutron guide tube bent in the vertical direction, having the form of a suspended chain. The use of two thin Ni-foils makes the design very economic and a concentration of low-energy neutrons achievable.
Experimental verification of the theoretical findings is in progress.

5.) Resonance Transmission of Gross Fission Product Mixtures (H.G.Priesmeyer)

Figure 3 shows the transmission of an irradiated Uranium sample from 3 eV to 140 eV, which had been irradiated for about 10 months in 1971/72. The U235 depletion of the high-enrichment MTR fuel (90 % U235) is 55 %.
The result has to be compared to earlier measurements of the same sample as well as to measurements of samples with different burnups. Since the fission product Kr-85 is in its formation maximum, the search for an identification of this isotope is carefully considered.

6.) Calculation and Measurement of the Transmission and Resolution of the Fast-Chopper (B.Asmussen, U.Harz, H.G.Priesmeyer)

The proven reliability of the cryogenic sample changer has encouraged future transmission resonance measurements to be performed with reduced Dopplerbroadening. In order to arrive at improved shape analysis of the data the chopper resolution has to be determined more realistically for the equipment now in use.

Publications

P. Fischer, U. Harz, H. G. Priesmeyer
The first (n,p) oscillator level in ZrH_x at low temperature
(presented at the Conference 'The Neutron and its Applications' Cambridge 1982, to be published).

H. G. Priesmeyer, P. Fischer, U. Harz, B. Soldner
Comparative measurements between a Li-6 glass and a He-3 high-pressure gas scintillator
(Nuclear Data for Science and Technology, Antwerp 1982, 880-882)
being published in a technically detailed version as GKSS-E report.

U. Harz, P. Fischer, H. G. Priesmeyer
Ein modernes System zur Messung und Auswertung von Neutronenflugzeitspektren.

P. Henkens, P. Fischer, U. Harz, H. G. Priesmeyer
Ein 24-keV Neutronenfilter am FR Geesthacht I.

H. G. Priesmeyer
Ein fokussierender Leiter für langsame Neutronen.

Deutsche Physikalische Gesellschaft
Münster, März 1983

Proton Cross Section at lHe-Temperature

11:21 Mi., 4. Mai 1983

IKK FAST CHOPPER		
Chopper Run	228-02	
Sample Thickn. H	0.032300	atoms/barn
Sample Thickn. Zr	0.016800	atoms/barn
Sigma-Korr	1.10	barn
Channel Width	6.40	microsec
Delay Time	2637.10	microsec
Flight Path	42.93	m

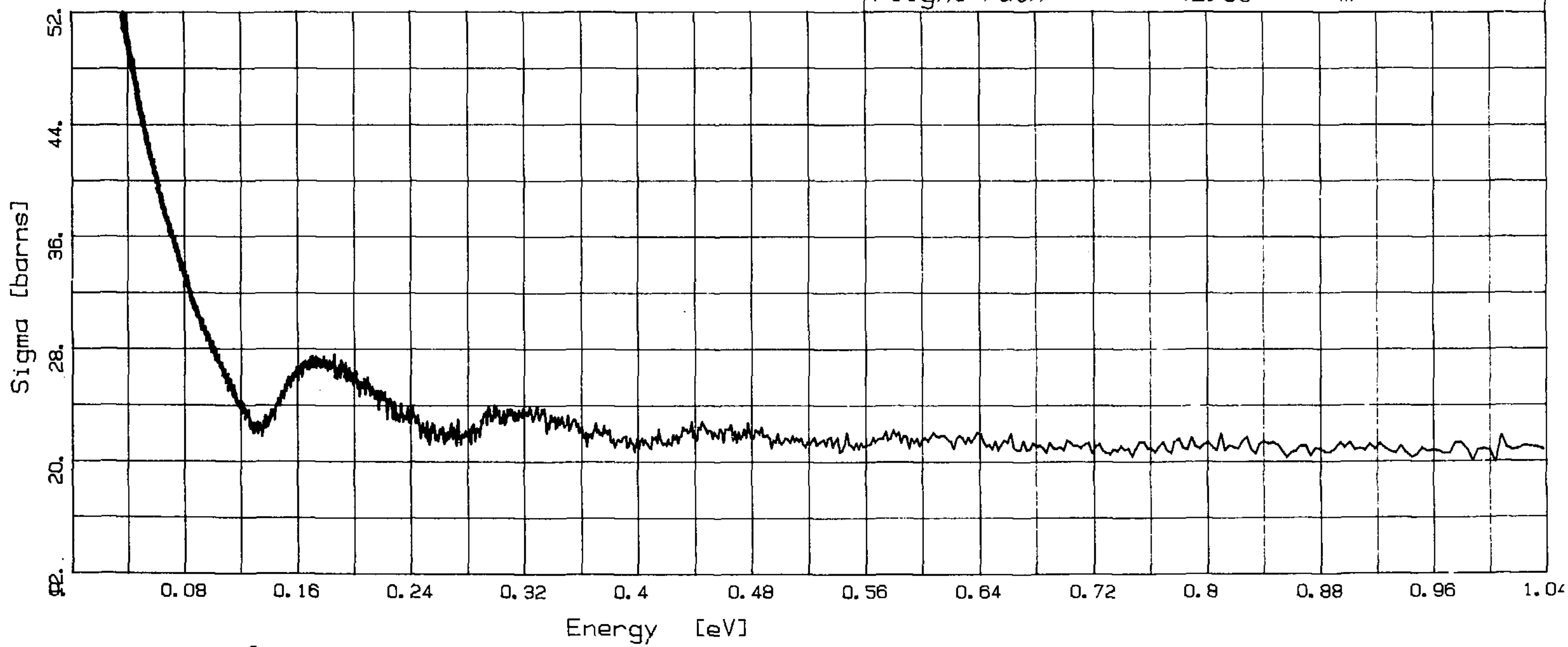

Mi., 30. Maerz 1983 EISENFILTER

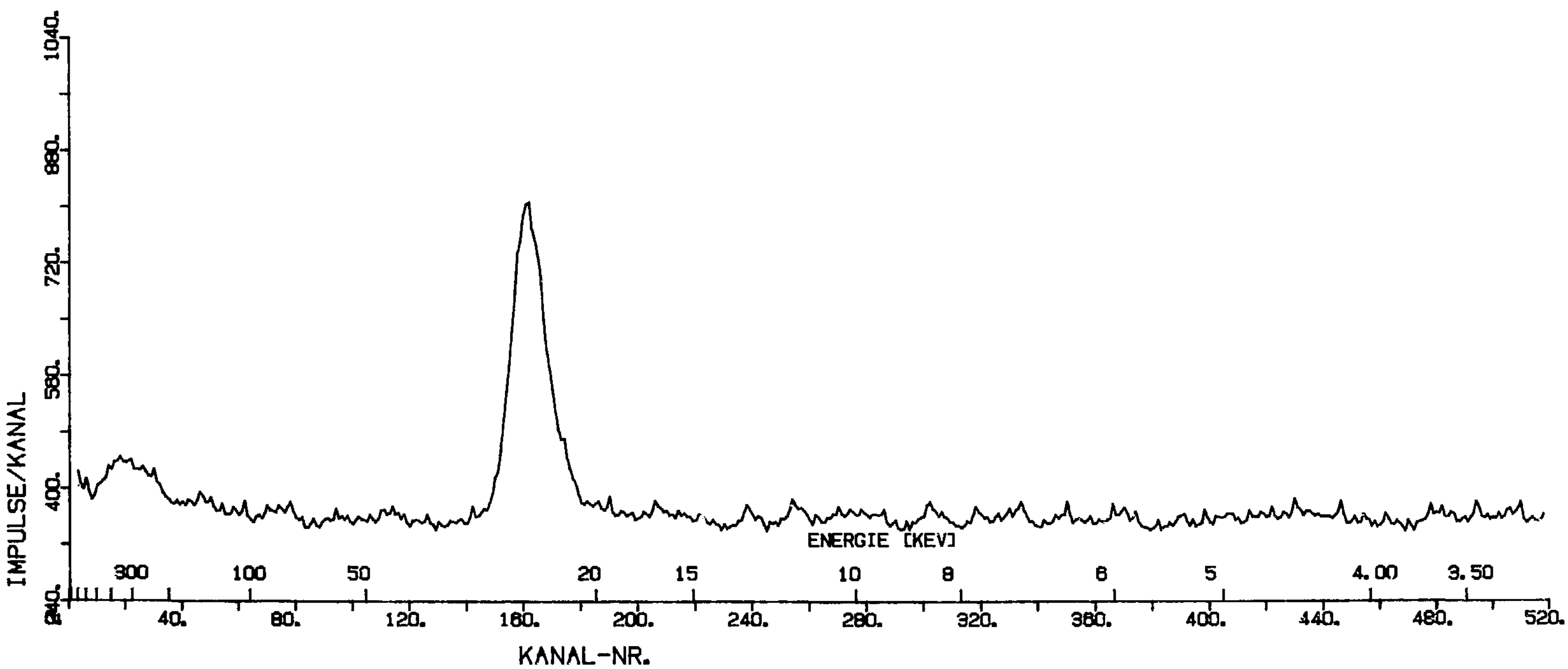

GFP-Transmission Probe 24 (3 - 140 eV)

15:57 Do., 28. April 1983

IKK FAST CHOPPER		
Chopper Run	230-01	
Sample Thickness	0.010000	atoms/barn
Rotor Speed	3750.00	rpm
Channel Width	0.60	microsec
Resolution	3.56	channels
Delay Time	253.06	microsec
Flight Path	42.93	m

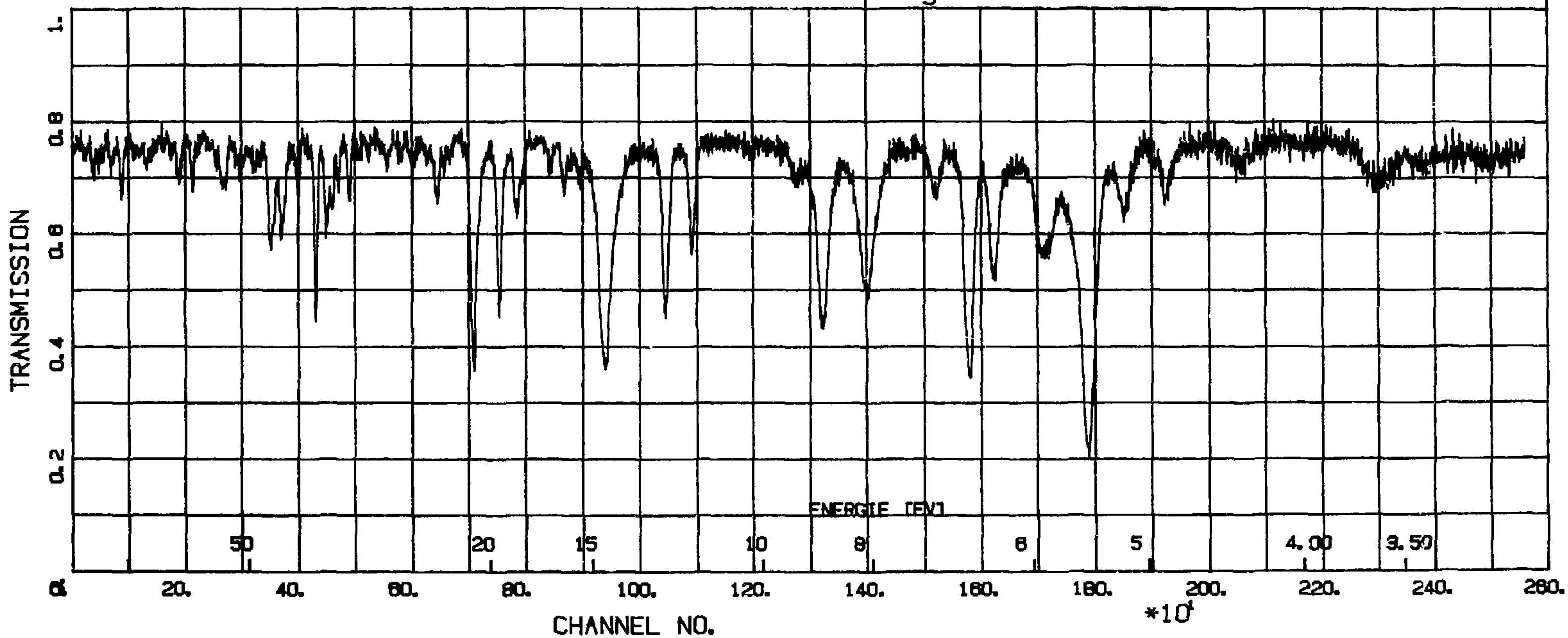

INSTITUT FÜR KERNCHEMIE
UNIVERSITÄT ZU KÖLN

1. Measurement and Theoretical Prediction of Integral Excitation Functions of Light Charged Particle Induced Reactions

R.Michel, M.Galas and R.Stück

1.1 Deuteron-Induced Reactions on Cobalt

While the hybrid model [1] of nuclear reactions in the form of OVERLAID ALICE [2] is well capable to predict unknown excitation functions of p-induced reactions up to 45 MeV [eg.3] the hybrid model analysis of integral excitation functions of α-induced reactions on elements from Ti to Ni showed severe shortcomings [4,5,6]. In order to clarify the observed discrepancies and to provide a systematic survey on the reactions of light charged particles we investigated d- and ^{3}He-induced reactions on Cobalt for $E/A \leqq 45$ MeV. Using the stacked foil technique integral excitation functions for the d-induced production of ^{57}Ni, ^{56}Ni, $^{60m+g}$Co, $^{58m+g}$Co, ^{57}Co, ^{56}Co, ^{55}Co, ^{59}Fe, ^{52}Fe, ^{56}Mn, ^{54}Mn, ^{52}Mn, ^{51}Cr, ^{48}V, ^{47}Sc and $^{46m+g}$Sc were measured for d-energies between 9 and 85 MeV [7]. The comparison of the experimental cross sections with a priori calculations showed that {(d,xpyn),x=0-7,y=0-8} reactions are well described by statistical plus preequilibrium (PE) theories of nuclear reactions. Calculations according to Weißkopf and Ewing [8] taking not into account PE effects showed that the excitation functions measured exhibit strong PE effects. The PE contributions can be well described in the framework of the hybrid using an initial exciton number between 2 and 3. Exemplarily, the good agreement between experimental and calculated excitation functions is shown in Fig.1.

The deviations between theory and experiment between 10 and 15 MeV in Fig.1 are due to the evaporation of ^{3}H which is not considered in the compound nucleus calculations. For d-induced reactions important discrepancies between experimental and calculated cross sections are only observed for the reaction ^{59}Co(d,p)$^{60m+g}$Co which is well known to be dominated by direct processes (Fig.2). Minor influences of direct reactions are also seen in the ^{59}Co(d,2p)^{59}Fe reaction resulting in an underestimation of the cross sections by theory. On the other hand the experimental data do not indicate an important contribution of PE emission of α-particles as observed earlier for p- and α-induced reactions

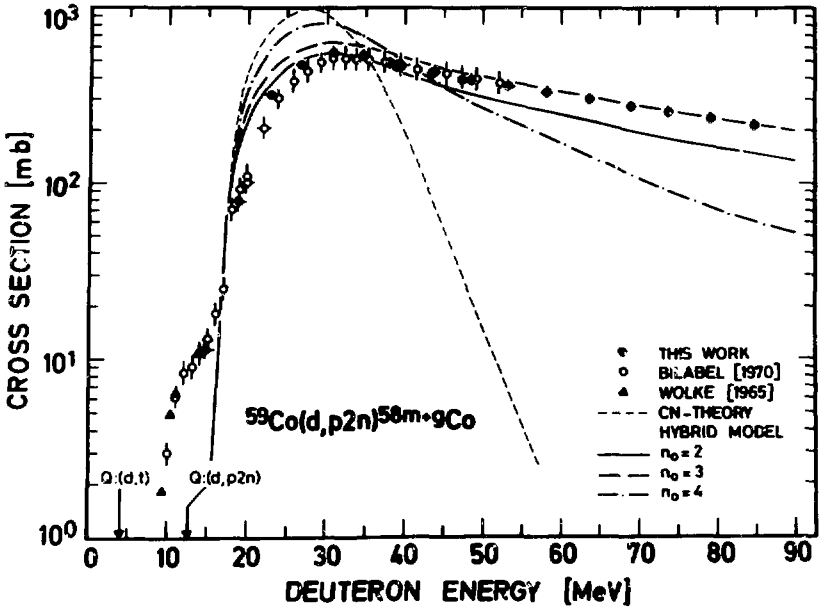

Fig.1: Experimental cross sections and hybrid model calculations for the reaction $^{59}Co(d,p2n)^{58m+g}Co$. For the work of other authors see [9,10].

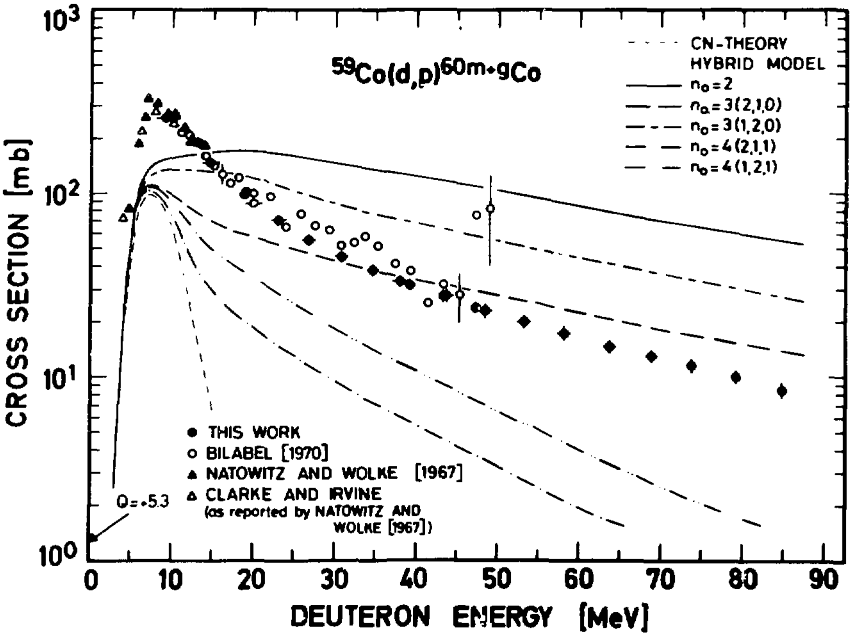

Fig.2: Experimental cross sections and hybrid model calculations for the reaction $^{59}Co(d,p)^{60m+g}Co$. For the work of other authors see [9,11].

[5,6,7,12]. Moreover it is point out that the hybrid model calculations of d-induced reactions on Co successfuly describe also product nuclides which in the energy range investigated are only produced by statistical processes if the general competition of PE decay is taken into account.

1.2 ^{3}He-Induced Reactions on Cobalt

19 excitation functions for the τ-induced production of ^{61}Cu, ^{57}Ni, $^{60m+g}$Co, $^{58m+g}$Co, ^{57}Co, ^{56}Co, ^{55}Co, ^{59}Fe, ^{56}Mn, ^{54}Mn ^{52}Mn, ^{51}Cr, ^{48}Cr, ^{48}V, ^{48}Sc, ^{47}Sc, $^{46m+g}$Sc, and ^{44m}Sc from cobalt were measured for τ-energies from 14 to 130 MeV [13]. Also for τ-induced reactions a detailed hybrid model analysis was performed. The excitation functions show strong contributions of PE effects up to reactions of the type (τ,4pxn). From the analysis of the reaction ^{59}Co(τ,n)^{61}Cu (Fig.3) an unambiguous choise of the initial exciton configuration is possible. It turns out to be n_o=4(1n-3p-0h). However the theoretical predictions for nearly all other reactions in particular for {(τ,2pxn),x=0,2,3}, (τ,3p) (Fig.4) and (τ,4p2n) show severe shortcomings. For the explanation of the observed discrepancies break up of the incoming ^{3}He particles as well as double stripping may be assumed. Moreover contributions of PE α-emission are seen giving rise to discrepancies between theory and experiment in the low energy part of the excitation functions. The results indicate that - as in the case of α-induced reactions - the initial states of ^{3}He-induced reactions are more complicated than assumed by the hybrid model [1] in the present form of OVERLAID ALICE [2].

1.3 Monitor Reactions for High Energy Protons: On the Consistency of the Excitation Functions for ^{27}Al(p,3pn)^{24}Na and ^{27}Al(p,3p3n)^{22}Na

Extending our earlier work on p-induced reactions on elements from Ti to Ni to p-energies up to 200 MeV several irradiation experiments were performed at the SC of the IPN Orsay. Since there were no Faraday cups available we had to monitor the p-beam current by monitoring reactions. As reference excitation function we used the "valeurs adoptêes" given by Tobailem and de Lassus St.Genies [14] for Al(p,3p3n)^{22}Na for p-energies from 80 to 200 MeV (Table 1). In the same Al foils we also measured the cross sections for the reaction ^{27}Al(p,3pn)^{24}Na,in order to check the consistency of these often used monitor excitation functions. The results

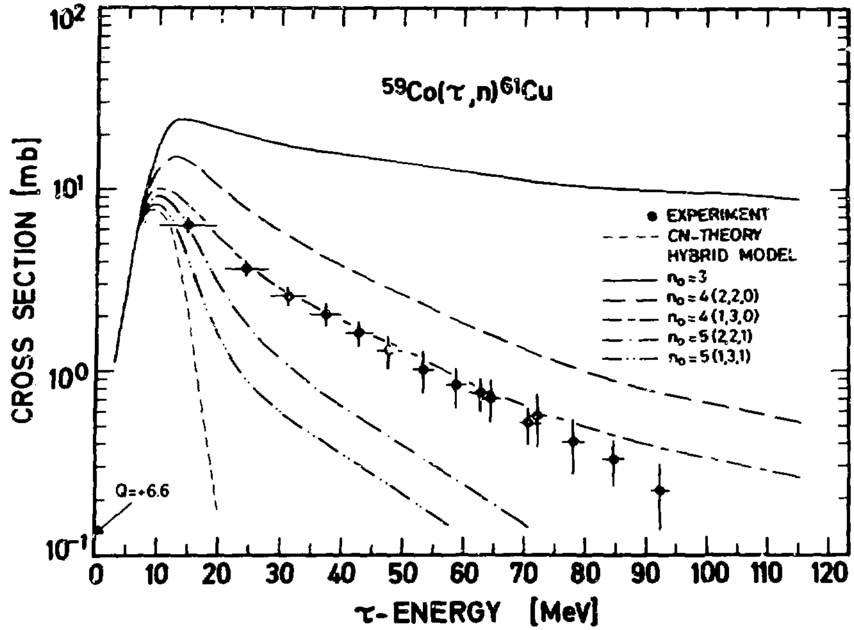

Fig.3: Experimental and theoretical excitation functions for the reaction $^{59}Co(\tau,n)^{61}Cu$.

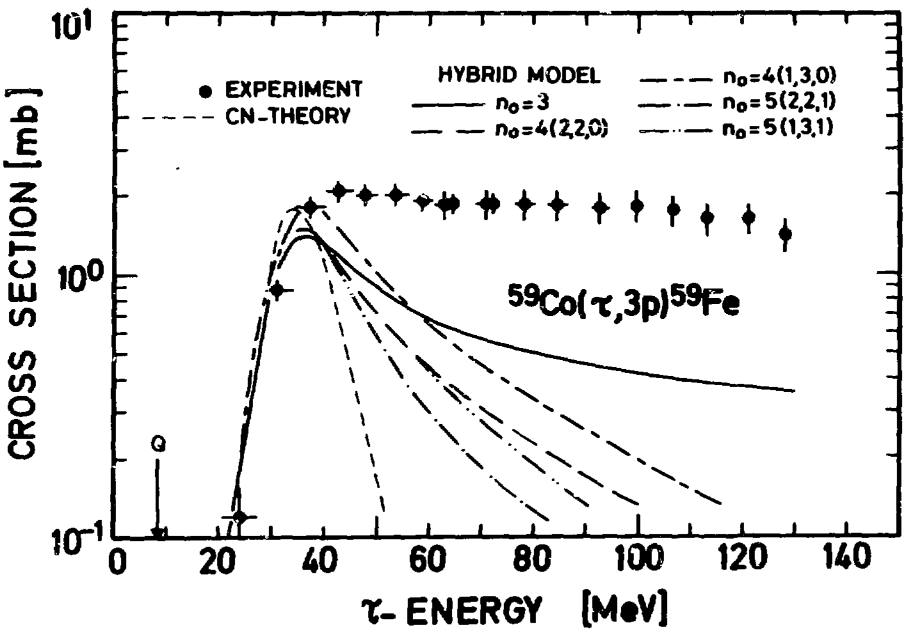

Fig.4: Experimental and theoretical excitation functions for the reaction $^{59}Co(\tau,3p)^{59}Fe$.

are presented in table 1. Using the $^{27}Al(p,3p3n)^{22}Na$ reaction as monitor reaction we obtained consistency between the two reactions for p-energies between 200 and 150 MeV on the basis of the values recommended in [14]. For energies below 150 MeV our cross sections for the production of ^{24}Na are significantly higher than the "valeurs adoptées" from Tobailem et de Lassus St.Genies [14], pointing to an inconsistency between the evaluated excitation functions for the production of ^{22}Na and ^{24}Na. Our measured $^{22}Na/^{24}Na$ ratios are lower than those of Tobailem and de Lassus St.Genies [14] by up to 20% between 80 and 120 MeV. However considering the absolute errors of about 10% for the ^{24}Na cross sections there are no significant discrepancies between our experimental data and the experimental data given by most of the other authors refered to in [14].

E_p [MeV]	^{22}Na	^{24}Na	E_p [MeV]	^{22}Na	^{24}Na
79 ± 2	21.6	12.1 ± 1.2	154 ± 2	15.9	9.97 ±0.90
89 ± 2	19.9	11.4 ± 1.1	161 ± 2	15.7	9.92 ±0.89
97 ± 2	19.0	11.0 ± 1.1	166 ± 2	15.6	9.96 ±0.98
107 ± 2	18.2	10.8 + 1.1	172 ± 2	15.4	9.82 ±0.88
115 ± 2	17.6	10.6 ± 1.1	178 ± 2	15.3	9.73 ±0.88
124 ± 2	17.1	10.7 ± 1.1	184 ± 2	15.2	9.64 ±0.87
132 ± 2	16.8	10.6 ± 1.1	189 ± 2	15.1	9.56 ±0.86
140 ± 2	16.4	10.5 ± 1.1	194 ± 2	15.1	9.58 ±0.86
148 ± 2	16.1	10.3 ± 1.0	199 ± 2	15.0	9.46 ±0.85

Table 1: Cross sections for the reactions $^{27}Al(p,3pn)^{22}Na$ adopted from [14] as monitor reaction and respective experimental cross sections for $^{27}Al(p,3p3n)^{24}Na$ from this work. The cross sections are given in [mb].

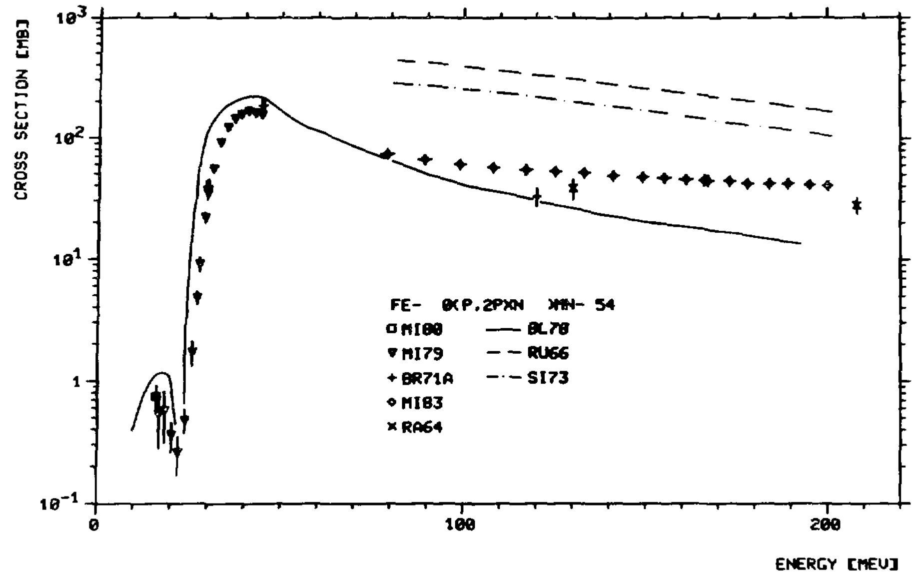

Fig.5: Comparison of experimental cross sections for Fe(p,2pxn)^{54}Mn with hybrid model calculations (BL78) and with estimates according to the semiempirical formulas of Rudstam (RU66) and of Silberberg and Tsao (SI73). The data of this work are labelled (MI83) [15]. For earlier work see [3,18,19,20].

1.4 Excitation Functions for p-Induced Reactions on Ti, Fe and Ni for p-Energies between 80 and 200 MeV

For the cosmochemical relevant target elements Ti, Fe and Ni we measured about 50 excitation functions for the production of radionuclides ($40 \leq A \leq 60$) for p-energies from 80 to 200 MeV [15]. In this energy region up to now only very few and partially strongly contradictory cross section measurements were available. The new data provide a basis for model calculations of the interaction of primary galactic protons with extraterrestrial matter [ibid]. At the same time they allow to evaluate the quality of theoretical estimates of unknown excitation functions, which are often used in cosmochemistry for this energy region. Therefore hybrid model calculations [1,2] were performed up to 200 MeV and, moreover, the experimental cross sections were estimated on the basis of the semi-empirical formulas of Rudstam [16] and of Silberberg and Tsao [17]. Exemplarily in Fig.5 and 6 excitation functions for Fe(p,2pxn)^{54}Mn and Fe(p,3pxn)^{51}Cr are shown. Generally the hybrid model calculations are in

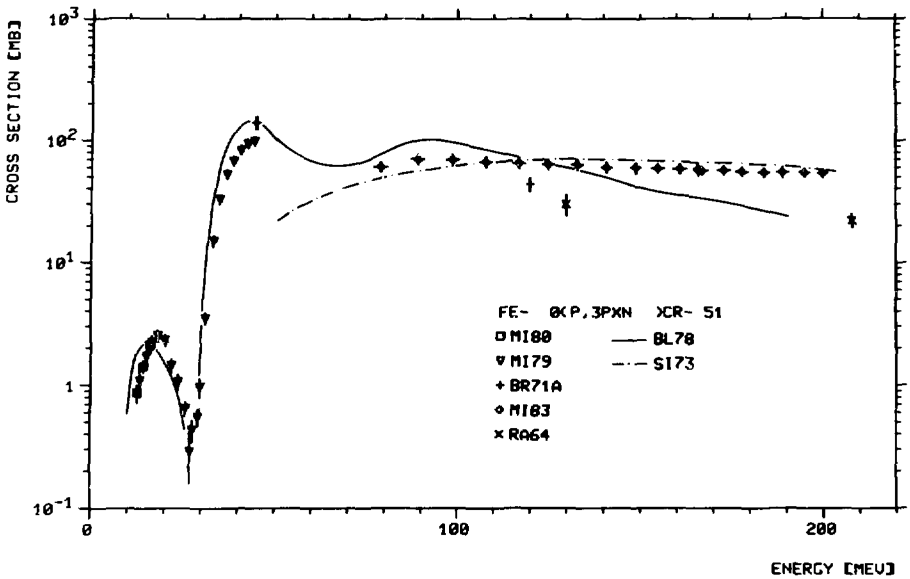

Fig.6: Comparison of experimental cross sections for Fe(p,3pxn)^{51}Cr with hybrid model calculations (BL78) and with estimates according to the semiempirical formula of Silberberg and Tsao (SI73). The data of this work are labelled (MI83) [15]. For earlier work see [3,18,19,20].

good agreement with the experimental data below 100 MeV. At present we are measuring excitation functions for these reactions also for p-energies from 45 to 80 MeV using the cyclotron at Louvain La Neuve. Preliminary data of this experiment strengthen the above statement.
For higher energies the calculations tend to underestimate the experimental data. Here the inclusion of multiple PE emission [21] possibly might improve the calculations in the future.

On the other hand the semiempirical formulas [16,17] give results of strongly varing quality. For the production of ^{54}Mn from Fe (Fig.5) which might be a little bit to close to the target they deviate from the experimental data considerably (Fig.5). For ^{51}Cr (Fig.6) both formular give identical results which are in good agreement with the measured cross sections. But generally there are no systematic trends in the agreement or in the discrepancies observed so that the use of these formulas for precise model calculations in cosmochemistry should be avoided.

References

[1] M.Blann, Phys.Rev.Letters 27 (1971) 337

[2] M.Blann (1978) UR-NSRL-181

[3] R.Michel, G.Brinkmann, H.Weigel, W.Herr, Nucl.Phys. A 322(1979)40

[4] R.Michel, G.Brinkmann, Nucl.Phys. A 338 (1980) 167

[5] R.Michel, G.Brinkmann, R.Stück, in: K.H.Böckhoff (ed.) Proc. of an Int.Conf. on Nuclear Data for Science and Technology, Sept.6-10, 1982 Antwerp, (1983) 599

[6] R.Michel, G.Brinkmann, R.Stück, Radiochimica Acta, (1983) accepted for publication

[7] R.Michel, M.Gallas, Int.J.Appl.Rad.Isotopes (1983) accepted for publication

[8] V.F.Weisskopf, D.H.Ewing, Phys.Rev.57 (1940) 472

[9] R.Bilabel, KFK 1171 (1970); Radiochemica Acta 15 (1971) 13

[10] R.L.Wolke, TID-21525 (Annual Rep.) Univ. of Pittsburgh (1965)

[11] J.B.Natowitz, R.L.Wolke, Phys.Rev. 155 (1967) 1352

[12] R.Michel, H.Weigel, W.Herr, Z.Phys. A 286 (1978) 393

[13] R.Michel, M.Gallas, Nucl.Phys.A (1983) accepted for publication

[14] J.Tobailem, C.H.de Lassus St.Genies, CEA - N - 1466 (3), (1975)

[15] R.Michel, R.Stück, Proc.14th Lunar Plan.Sci.Conf., J.Geophys. Res. (1983) submitted

[16] G.Rudstam, Z.Naturf. 21a (1966) 1027

[17] R.Silberberg, C.H.Tsao, Astrophys.J.Suppl.25 (1973) 315, 335

[18] R.Michel, G.Brinkmann, J.Radioanal.Chem. 59 (1980) 467

[19] R.L.Brodzinski, L.A.Rancitelli, J.A.Cooper, N.A.Wogman, Phys.Rev. C4 (1971) 1257

[20] G.V.S.Rayudu, Can.J.Chem. 42 (1964) 1149

[21] M.Blann, J.Bisplinghoff, UCID-19614 (1982)

INSTITUT FÜR KERNCHEMIE
JOHANNES GUTENBERG-UNIVERSITÄT MAINZ

Measurement of the absolute γ-ray line intensities in the mass chains 144, 146, and 147 at the mass separator OSTIS

B. Sohnius, B. Pfeiffer, H.O. Denschlag

Unknown absolute γ-ray line intensities of the early members (barium, lanthanum, and cerium) in mass chains 144, 146, and 147 were determined relative to the absolute γ-ray line intensities of the well known descendants La-144, Pr-146, and Pr-147 using the mass separator OSTIS of ILL, Grenoble.

The method relies on a clean chemical separation of the first chain members of interest (Cs and Ba) from their descendants that takes place in the ion source of the separator.

The separation is based on the different volatilization temperatures rising drastically in the sequence Cs < Ba < (La, Ce, Pr). The cleanliness was tested by measuring the relative count rates (I_x) of Cs, Ba, and La at various heating currents in the ion source. The measurements were carried out under radioactive equilibrium conditions.

Fig. 1 shows that the ratio I_{Ba}/I_{Cs} increases slightly with rising temperatures and indicates that barium is starting to contribute to the beam which is principally cesium. On the other hand, the ratio I_{Ba}/I_{La} that remains constant (Fig. 1) indicates no volatilization of rare earths.

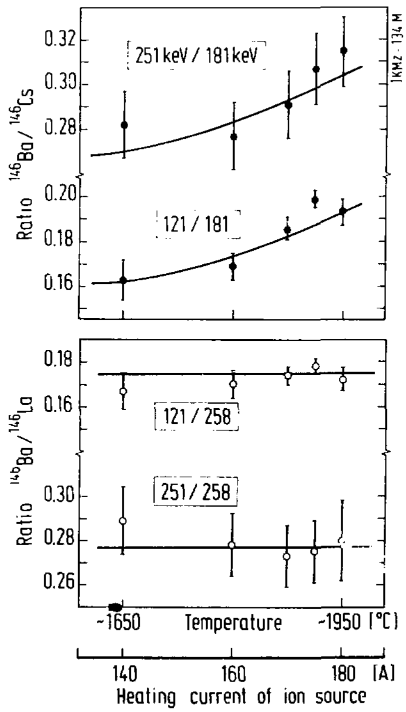

Fig. 1: Ratio of Cs, Ba and La count rates vs heating current of ion source resp. approximate ion source temperature

Table 1: γ-ray line intensities in chains 144, 146, and 147

Nuclide	E_γ (keV)	I_γ^{rel} (%)	I_γ^{rel} (%)	I_γ^{rel} (%) (this work)	I_γ^{abs} (%)
Ba-144	103.4	100 [1]		100	27.1 ± 2.7
La-144	397.3*	100			90.33 [2]
Ba-146	140.7	100 [2]	100 [3]	100	22.6 ± 3.0
Ba-146	251.1	100	98 ± 4	83 ± 8	18.0 ± 2.0
Ba-146	121.0	93	67 ± 4	63 ± 6	14.2 ± 1.4
Ba-146	197.0	65	62 ± 3	56 ± 5	12.7 ± 1.3
La-146	258.5	1000 [8]	1000 [4]	1000	63.7 ± 3.0
La-146	924.6	123	127	121 ± 10	7.7 ± 0.8
La-146	702.3	100	90	101 ± 3	6.4 ± 0.6
La-146	666.1	98	93	90 ± 3	5.7 ± 0.6
Ce-146	316.7	100 [5]		100	56.2 ± 3.0
Pr-146	453.9*	100			48.0 [6]
La-147	117.6	100 [9]	100 [10]	100	12.7 ± 1.2
La-147	186.9	28	53	68 ± 4	8.6 ± 0.5
La-147	438.4	19	43	43 ± 4	5.5 ± 0.5
La-147	235.7	11	23	23 ± 2	2.9 ± 0.3
Ce-147	268.7	61 [9]		61	6.3 ± 1.0
Pr-147	314.6*	100			12.6 [7]

*Reference line

The evaluation of the γ-ray spectra measured at an ion source temperature of ∿1910 °C was made using the Mainz computer program (Cal). Complex γ-ray peaks were corrected using clean γ-lines of the contaminants.

The results for the strongest γ-lines are listed in Table 1. General agreement is found between our values and those found in the literature for the relative line intensities including those not listed in the table. A discrepancy for ^{147}La seems to have been settled in favour of Ref. [10] by the present measurements.

References

[1] J.K. Tuli, Nucl. Data Sheets 25, 53 (1978)

[2] J. Blachot, C. Fiche, Atomic Data and Nuclear Data Tables 20/3, 241 (1977)

[3] B. Sohnius, H, Braun, H.O. Denschlag, W. Pörsch, H. Faust, LOHENGRIN Data for A = 146, unpublished

[4] E. Monnand, private Communication (1982)

[5] H. Yamamoto, Y. Ikeda, K. Kawade, T. Katoh, T. Nagahara, J. Inorg. Nucl. Chem. 42, 1539 (1980)

[6] H.W. Taylor, B. Singh, J. Phys. G3, 1577 (1977)

[7] J.A. Pinston, R. Roussille, G. Bailleul, J. Blachot, J.P. Boquet, E. Monnand, B. Pfeiffer, H. Schrader, F. Schussler, Nucl. Phys. A246, 395 (1975)

[8] G.M. Gowdy, R.E. Chrien, Y.Y. Chu, R.L. Gill, H.J. Liou, M. Shmid, M.L. Stelts, K. Sistemich, F.K. Wohn, H. Yamamoto, D.S. Brenner, T.R. Yeh, R.A. Meyer, C. Chung, W.B. Walters, R.F. Petry, Proc. 4th Int. Conf. on Nuclei far from Stability, Helsingør 1981, CERN Rep. 81-09 (1981), p. 562

[9] F. Schussler, B. Pfeiffer, H. Lawin, E. Monnand, J. Münzel, J.A. Pinston, K. Sistemich, Proc. 4th Int. Conf. on Nuclei far from Stability, Helsingør 1981, CERN rep. 81-09 (1981), p. 589

[10] M. Shmid, Y.Y. Chu, G.M. Gowdy, R.L. Gill, H.J. Liou, M.L. Stelts, R.E. Chrien, R.F. Petry, H. Dejbakhsh, C. Chung, D.S. Brenner, Proc. 4th Int. Conf. on Nuclei far from Stability, Helsingør 1981, CERN rep. 81-09 (1981), p. 576

INSTITUT FÜR KERNCHEMIE

PHILIPPS-UNIVERSITÄT MARBURG

1. Gamma-Ray Catalog

U. Reus, W. Westmeier

Quantitative information on gamma rays from the decay of radioactive nuclides is required in many areas of nuclear science as well as related fields. We have therefore produced a compilation of the decay properties of all known radionuclides, with the main emphasis on energies and absolute intensities of gamma rays. A first printed version of this catalog was issued in 1979, covering references to the literature through June 1978.

Revision of data for a second edition has now been completed, and includes references through June 1982. The updated version contains information on 2526 nuclides and isomers with a total of more than 47,000 gamma rays and X-rays, the information on X-rays accompanying radioactive decay being a newly introduced feature. As before, the catalog will be presented in two parts: In Part I gamma rays are listed in order of increasing energy for the purpose of identification of unknown gamma lines. In Part II complete data-sets for each nuclide are listed in order of mass number A and nuclear charge Z of the nuclides. This part also contains additional information, references, and comments in case of any discrepancies.

Preparations for publication of the second edition have recently been completed. The catalog is scheduled to appear in "Atomic Data and Nuclear Data Tables", Volume 29, which is to be issued in the second half of 1983.

2. Alpha-Energy Table

W. Westmeier, R.A. Esterlund

A compilation of alpha-decay properties of all known alpha-emitting nuclides, which includes data on alpha energies, intensities, and the abundance of the alpha branch, is permanently being updated. The table is ordered by increasing energy and covers data on 534 alpha emitters with a total of 1621 energies at present.

Computer printout copies of the table are available on request.

REAKTORSTATION GARCHING; FACHBEREICH PHYSIK
TECHNISCHE UNIVERSITÄT MÜNCHEN

1. Coherent Neutron Scattering Lengths

1.1. Scattering of Slow Neutrons by Lanthanium and Cerium

K. Knopf, W. Waschkowski

In continuation of our earlier studies on coherent bound scattering lengths b and on free scattering cross sections σ_0 [4] we performed measurements on isotopically enriched compounds of Lanthanium and Cerium. We obtained by means of Christiansen filter technique and transmission measurements the following data [1]:

$b(^{nat}La) = 8.24\ (4)$ fm , $\sigma_0(La, E=0) = 10.02\ (22)$ b ,
$b(^{nat}Ce) = 4.84\ (2)$ fm , $\sigma_0(Ce, E=0) = 3.01\ (5)$ b ,

$b(^{136}Ce) = 5.76\ (9)$ fm ,
$b(^{138}Ce) = 6.65\ (9)$ fm ,
$b(^{140}Ce) = 4.81\ (9)$ fm ,
$b(^{142}Ce) = 4.72\ (9)$ fm.

By comparison with the resonance parameters we derived the free potential radii R' and the spin state scattering lengths b_+ und b_-
for ^{139}La : R' = 4.6 (2) fm and $b_+ = 11.4\ (3)$ fm
$b_- = 4.5\ (4)$ fm and
for ^{136}Ce : R' = 5.3 (2) fm ,
for ^{140}Ce : R' = 5.6 (2) fm ,
for ^{142}Ce : R' = 5.5 (3) fm.

1.2. Neutron Scattering Length of Lithium and Boron

L. Koester, K. Knopf, W. Waschkowski

By means of Christiansen filter technique coherent bound scattering lengths were determined and by comparison with free cross sections from transmission measurements we derived the scattering lengths of the isotopes of Li and B.

We used 15 different samples of Li-compounds to obtain the complex spin state scattering lengths for the bound atom:

$$^{6}\mathrm{Li}: \quad b_+ = 0.67(14) - i\cdot 0.08(1)\ \mathrm{fm}$$
$$b_- = 4.67(17) - i\cdot 0.62(2)\ \mathrm{fm}$$

$$^{7}\mathrm{Li}: \quad b_+ = -4.15(6)\ \mathrm{fm}$$
$$b_- = 1.00\ (8)\ \mathrm{fm}$$

Measurements on 3 boron samples with different isotopical enrichments led to

for ^{10}B : $b_+ = -4.2(4)$ fm, $\quad b_- = 5.2(4)$ fm

for ^{11}B : $b_+ = 5.6(3)$ fm, $\quad b_- = 8.3(3)$ fm

A rewiew on slow neutron scattering and resonance data showed an over all consistency of all values [2] .

1.3 Scattering Lengths of some Molten Metals

L. Koester, G. Reiner, W. Waschkowski

Using the gravity refractometer neutron reflection measurements on mirrors of molten metals led to coherent bound atom scattering lengths with high accuracy as follows [3] :

Ga : $b = 7.2879\ (16)$ fm,
Sn : $b = 6.2257\ (19)$ fm,
Tl : $b = 8.7756\ (45)$ fm,
Pb : $b = 9.4054\ (27)$ fm,
Bi : $b = 8.5313\ (20)$ fm.

The new value for Bi differs about 3 standard deviations from the recommended standard value for scattering length in [5] .

References

[1] K. Knopf, W. Waschkowski, Streuung langsamer Neutronen an Lanthan und Cer.
Z. Naturforschung 37a, 1132-1138 (1982)

[2] L. Koester, K. Knopf, W. Waschkowski, Neutron Scattering Length of Lithium and Boron.
submitted to Z. f. Physik A

[3] L. Koester, G. Reiner, W. Waschkowski
to be published in a short time.

[4] L. Koester, Neutron Scattering Lengths and Fundamental Neutron Interactions.
Springer Tracts in Modern Physics, Vol. 80, 1-55, (1977)
Berlin, Heidelberg, New York: Springer.

[5] S.F. Mughabghab, M. Divadeenam, N.E.Holden, Neutron cross sections Vol.1., Part A, Academic Press New York, London (1981).

INSTITUT FÜR KERNENERGETIK UND ENERGIESYSTEME (IKE)
UNIVERSITÄT STUTTGART

1. Nuclear Data Processing

J. Keinert, M. Mattes, W. Speyer

The activities at IKE in the field of nuclear data are mainly concerned with the processing of evaluated nuclear data for application in nuclear engineering. This includes

- test and comparison of different evaluated nuclear data sets also in graphical form and check against resonance integral and spectrum averaged data
- updating of evaluated data sets if necessary
- generation of multigroup cross setion libraries in various energy group structures for neutrons and photons as well as coupled neutron and photon data sets with KERMA factors, damage cross sections and flux-to-dose rate conversion factors
- benchmark calculations for validation of generated multigroup data
- further development and updating of our retrieval- and processing code system for nuclear data

The following reports or technical notes were published:

J. Keinert: IKE Scattering Law Data Library in ENDF/B Format
IKE 6-TN-10 (1982)

J. Keinert, W. Speyer: GAMMA-36, a Multigroup Photon Cross Section Library based on VITAMIN-C in RSYST1 Format including KERMA Factors
IKE 6-TN-12 (1982)

M. Mattes, J. Keinert, W. Speyer: RESBIB-8500, a Neutron Cross Section Library for Isotopes of U, Pu and Gd in the Resonance Region (8500 Energy Groups up to 4.3 keV) based on ENDF/B-V and -IV
IKE 6-146 (1982)

M. Mattes, J. Keinert, W. Speyer: GAMMA-36C, a Multigroup Photon Cross Section Library up to P_8 based on ENDF/B Tapes 420 and 421 (Coherent Scattering considered) in RSYST1 Format including KERMA Factors
IKE 6-145 (1982)

M. Mattes: Graphical Presentation of Actinide Neutron Cross Sections from ENDF/B-V for Isotopes given in INDL/A Rev.6 (1982)
IKE 6-TN-16 (1982)

M. Mattes: Graphical Presentation of Actinide Neutron Cross Sections from INDL/A Rev. 6 (Files 1 - 4) for the Complete Energy Range
IKE 6-TN-17 (1982)

M. Mattes, J. Keinert: Comparison of Thermal Neutron Cross Sections, WESTCOTT g-Factors, and Resonance Integrals for ^{233}Pa, ^{237}Np, ^{242}Pu, ^{241}Am, ^{242m}Am, ^{243}Am, ^{242}Cm, ^{244}Cm, ^{245}Cm, ^{246}Cm, and ^{248}Cm from the Evaluated Neutron Data Files INDL/A (May 1982) and ENDF/B-V
IKE 6-TN-18 (1982)

M. Mattes, J. Keinert: Comparison of One Group Constants of the Nuclides ^{233}Pa, ^{237}Np, ^{242}Pu, ^{241}Am, ^{242}Am, ^{242m}Am, ^{243}Am, ^{242}Cm, ^{244}Cm, ^{245}Cm, and ^{246}Cm for different Neutron Spectra. (Data Bases: INDL/A-82 and ENDF/B-V)
IKE 6-TN-19 (1982)

J. Keinert: Vergleich von Neutronen-Wirkungsquerschnitten in THERM-126 Gruppenstruktur (Basis ENDF/B-V und -IV)
IKE 6-TN-25 (1983)

2. Adjustment of Neutron Multigroup Cross Sections to Deep Penetration Integral Experiments

G. Hehn, R.D. Bächle, G. Pfister, M. Mattes, W. Matthes[+]

Further progress has been achieved with the "global detector concept". Adjusted cross sections and covariance matrices are presented and discussed at the 6th Int. Conf. on Radiation Shielding (ICRS) at Tokyo, Japan, May 16-20, 1983.

[+] JRC EURATOM, Ispra/Italy

3. Modification of the low frequency distribution model for H bound in H_2O

J. Keinert

To take care of the temperature dependence of low energy motions of hydrogen bound in water, the phonon spectrum model /1/ for the hindered rotations and the translational motion was modified. In Fig. 1 some results are presented. The new model contains modified HAYWOOD/PAGE /2/ distributions for the acoustic modes at 295 K/550 K allowing interpolation for working temperature. The translational unit also is assumed to be temperature dependent taking into account clusters of H_2O molecules in the liquid phase.

This revised frequency distribution will be used for updating the IKE Scattering Law Data Library in ENDF Format.

References

/1/ Keinert, J.: THERM-126, a Thermal Neutron Cross Section Library including Scattering Matrices
IKE 6-105/1 (1978)

/2/ Page, D.I., Haywood, B.C.: The HARWELL Scattering Law Programme: Frequency Distributions of Moderators.
AERE-R 5778 (1968)

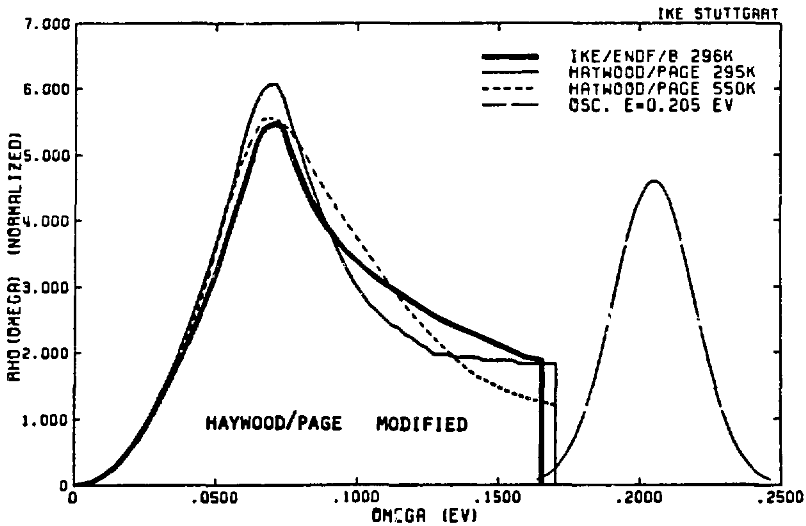

Fig. 1 LOW ENERGY FREQUENCY SPECTRA OF H BOUND IN LIQUID WATER

INSTITUT FÜR STRAHLENPHYSIK
UNIVERSITÄT STUTTGART

Measurement of Fast Neutron Cross Sections for the Reactions $^{27}Al(n,\alpha)^{24}Na$ and $^{27}Al(n,\alpha)^{24m}Na$ in the Energy Range 6.3 to 8.3 MeV

W.Enz, D.Kollewe and K.-W.Hoffmann

Cross sections for $^{27}Al(n,\alpha_o)^{24}Na(T_{1/2} = 900$ min) and $^{27}Al(n,\alpha_o)^{24m}Al(T_{1/2} = 20$ ms) reactions have been measured using the activation method. Fast neutrons were generated at the Stuttgart University 4 MV Dynamitron accelerator via the reaction $^{9}Be(\alpha,n)^{12}C$ using a 0.52 µm beryllium target on a water cooled copper backing /1/. The neutron flux was measured with a 2" x 2"-Ne 213 liquid scintillator cell allowing good neutron-gamma separation by a pulse shape discriminator. Spectrometry of reaction specific gamma rays was achieved by means of a calibrated Ge(Li)-detector.

In the selected energy range two neutron groups with Q-values 5,702 MeV and 1,263 MeV are produced in the $^{9}Be(\alpha,n)^{12}C$ reaction. The lower energy neutron group did not contribute to the activation, because the energy was always lower than the effective reaction threshold of the $^{27}Al(n,\alpha_o)^{24}Na$ reaction. Therefore activation was achieved only by the monoenergetic high energy neutron group. For the measurement with ^{24}Na in the ground state as residual nucleus the aluminum sample was mounted either at 90° or at 0° with respect to the DC alpha beam (average current 200 µA). After each activation cycle the sample was taken out of the target room and mounted in front of the Ge(Li)-detector. The cross section for the reaction to the 20 ms isomeric state ^{24m}Na was measured by means of a pulsed beam with the sample fastened in front of the well shielded Ge(Li)-detector in the target room.

The neutron flux monitor was mounted behind a collimator at 90° to the target. The flux at 0° was calculated via the angular distribution of the $^{9}Be(\alpha,n)^{12}C$ reaction. The efficiency of the scintillation cell was calculated with the program NEFF 4 of Dr. G.Dietze /2/, PTB Braunschweig.

Results of the cross section measurements are given in table 1. For the energies 7.9 MeV and 8.1 MeV the values for the $^{27}Al(n,\alpha_o)^{24}Na$ reaction were measured with the DC beam as well with the pulsed beam (P). Fig.1 shows our results together with the results of Liskien /3/, /4/ and Mostafa /5/ for the $^{27}Al(n,\alpha_o)^{24}Na$ reaction. To our knowledge the cross section for the $^{27}Al(n,\alpha_1)^{24m}Na$ reaction has been measured here for the first time in this energy region.

REACTION	MEAN NEUTRON ENERGY/MEV	ENERGY SPREAD MEV	CROSS SECTION MILLI BARN
$^{27}Al(n,\alpha_o)^{24}Na$	6.36	0.16	4.2 ± 0.4
	6.56	0.16	7.4 ± 0.8
	6.74	0.16	10.7 ± 1.1
	6.93	0.16	16.1 ± 1.7
	7.90	0.14	36.9 ± 4.2
		0.13	38.1 ± 4.7 (P)
	8.10	0.13	40.5 ± 4.6
		0.12	43.8 ± 5.4 (P)
	8.29	0.13	48.9 ± 5.5
$^{27}Al(n,\alpha_1)^{24m}Na$	7.90	0.13	14.5 ± 2.0
	8.10	0.12	19.9 ± 2.8

Table 1: Results of cross section measurements for the reactions $^{27}Al(n,\alpha_c)^{24}Na$ and $^{27}Al(n,\alpha_1)^{24m}Na$;(P): measured in connection with cyclic activation by a pulsed beam

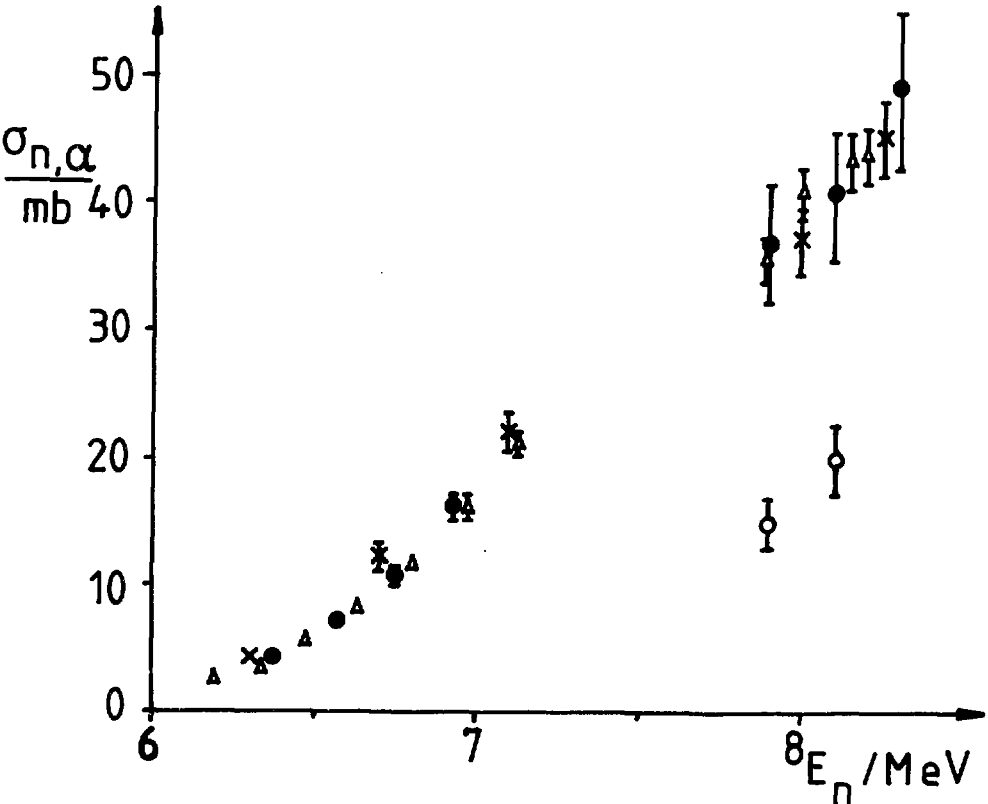

Figure 1: Cross sections for the reactions $^{27}Al(n,\alpha_o)^{24}Na$ (●) and $^{27}Al(n\,\alpha_1)^{24m}Na$ (o) as compared with the results of Liskien (▲) /3/, /4/ and Mostafa (x) /5/.

References:

/1/ J.W.Hammer and W.Nießner, Kerntechnik No. 11, 17 (1975)

/2/ G.Dietze, PTB-Bericht ND-22, PTB Braunschweig (1982)

/3/ H.Liskien and A.Paulsen, Nukleonik 8, 315 (1966)

/4/ S.Tagesen und H.Vonach, Physik-Daten - Physics Data 13-3, Fachinformationszentrum Karlsruhe (1981)

/5/ A.B.G.M.Mostafa, Nuclear Science and Applications, Vol.9, Ser. B (1976)

Investigation of Analyzing Power and Differential Cross Section of Calcium, Silicon, Sulfur, Yttrium and Lanthanium

G.Bulski, W.Grum, J.W.Hammer, K.-W.Hoffmann, H.Postner, G.Schleußner, E.Speller

Universität Stuttgart
Institut für Strahlenphysik
Allmandring 3
D-7000 Stuttgart 80
Federal Republic of Germany

Experimental Results.

For some medium weight nuclei analyzing power and differential cross section have been determined in one scattering experiment simultaneously. Details of experimental setup and procedure of measurement see[1].

For the elements Ca, Si, S and Y the neutron energy has been 7.75 MeV and the polarization of the neutrons has been 60%. For Lanthanum we produced neutrons with an energy of 8.73 MeV, for which we had to apply the full voltage of the Dynamitron accelerator, 4.05 MeV. The polarization degree of the neutrons was 40%. Experimental data at E_n = 7.75 MeV exist already.

Fig. 1 shows the analyzing power of Calcium corrected for finite geometry effects including multiple scattering. This angular distribution cannot be explained with any of the published sets of optical model parameters. The reason will be investigated further.

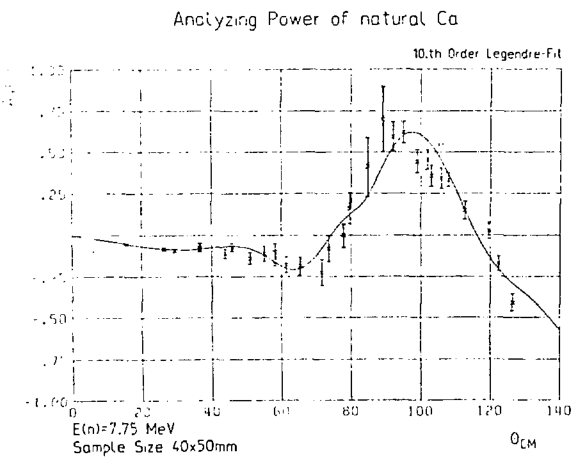

Fig. 1 Analyzing power of Ca at E_n = 7.75 MeV

For Silicon and Sulfur it was possible for the first time to evaluate also the inelastic scattering due to the improvements of the unfolding procedures.

Fig. 2 shows the analyzing power for Silicon for elastic and inelastic scattering.

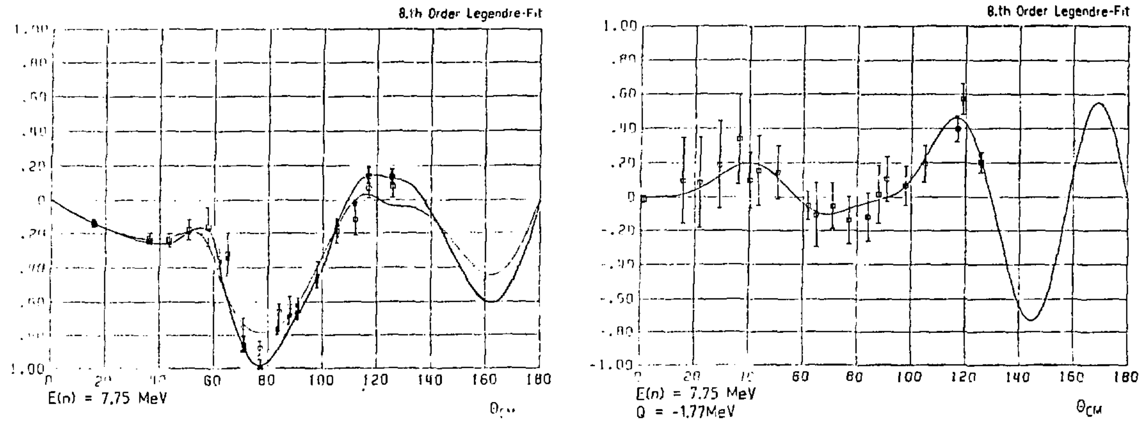

Fig. 2 Analyzing power of natural Silicon, E_n = 7,75 MeV
elastic scattering and inelastic scattering

The experimental results for Sulfur are given in Fig. 3.

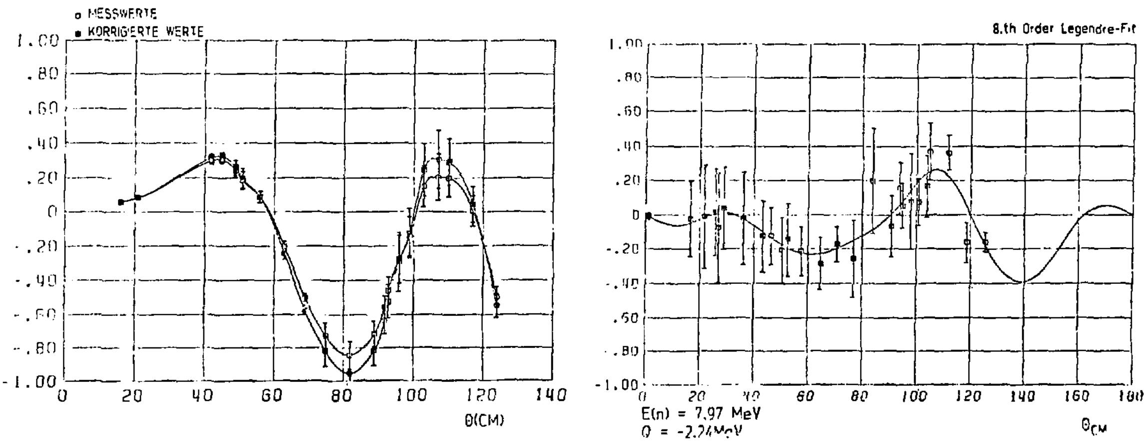

Fig. 3 Analyzing power of natural Sulfur, E_n = 7,75 MeV
elastic scattering and inelastic scattering

Technical improvements of the experiment and the evaluation

The revision of the unfolding procedure has been completed. A new unfolding code FANTI has been written, based on the known old codes FERDOR and FORIST. The response-matrix has been calculated for our detector geometry using the code NRESP 4 of Dietze[2] and using the most recent cross section data for Hydrogen and Carbon. Fig. 4 shows an example for an unfolding of a proton recoil spectrum under worst case conditions.

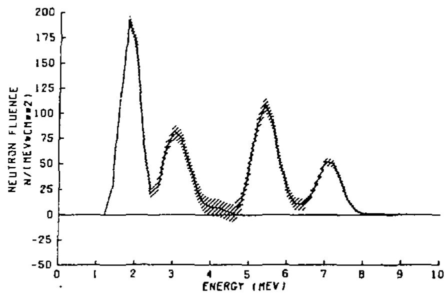

Fig. 4 Unfolded spectrum of neutrons scattered by Silicon at $\Theta = 110°$ near the minimum of the differential cross section with bad statistics. Elastic and inelastic scattered neutrons can be well separated nevertheless.

For the collection and storage of all the data of the scattering experiment a new microprocessor-system with adequate software has been installed and successfully used.

[1] K.H.Böckhoff (ed.) Proc. of Int. Conf. on Nuclear Data for Science and Technology, Antwerp 1982, page 783-791, Reidel, Dordrecht, Boston and London

[2] G.Dietze and H.Klein, PTB-report ND22

PHYSIKALISCH-TECHNISCHE BUNDESANSTALT
BRAUNSCHWEIG

1.1. Radionuclide Data

1.1 Half-Lives

K.F. Walz, H. Schrader

Half-lives of some radionuclides were determined by following the decay of encapsulated sources with a high pressure 4πγ ionization chamber. The results are summarized in Table I. Uncertainties (in parentheses) correspond to one standard deviation. The measuring period t is given as ratio to the half-life $T_{1/2}$. The sources were checked for impurities by germanium detector measurements.

The Half-Life of ^{90}Sr

H. Ramthun

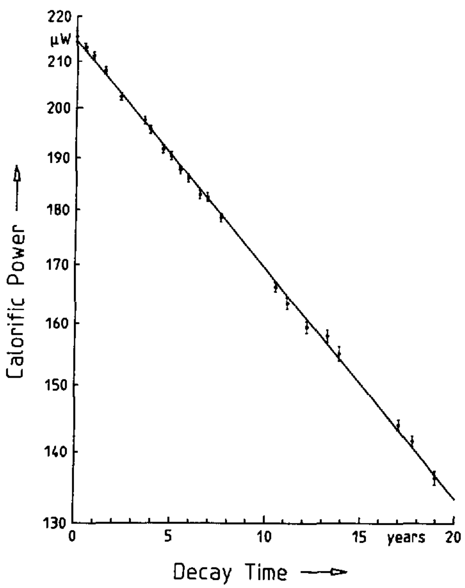

Fig. 1
Results of the heat power measurements as a function of the decay time

In the time between 1963 and 1982, 22 heat power measurements of a sealed $^{90}Sr/^{90}Y$ source were performed at the PTB by means of a twin-type calorimeter. The measured values with error bars at the 2 σ level are represented in fig. 1 as a function of time. From the straight line fitted to the measured values the following values were obtained for the half-life and its standard deviation

$T_{1/2}$ = (28.99 ± 0.25) years.

1.2 Gamma-Ray Emission Probabilities

U. Schötzig

Gamma-ray emission probabilities p of ^{169}Yb and ^{192}Ir were determined by using sources of known activity and calibrated Ge(Li) and high purity germanium spectrometers. The results are summarized in Table II. Uncertainties (in parentheses) correspond to one standard deviation.

Table I. Half-lives

Nuclide	$t/T_{1/2}$	$T_{1/2}$
^{57}Co	4.5	271.84(4)d
^{75}Se	2.2	119.76(5)d
^{90}Sr	0.1	10900(90)d
^{99}Mo	4.9	2.7476(5)d
$^{99}Tc^{m}$	9.7	0.25026(3)d
^{125}Sb	1.8	1008.1(8)d
^{144}Ce	2.5	284.45(14)d

Table II. Gamma-ray emission probabilities

^{169}Yb		^{192}Ir			
Energy in keV	p in %	Energy in keV	p in %	Energy in keV	p in %
20.8	0.19(2)	136.3	0.23(2)	484.6	3.20(3)
63.1	44.7(6)	201.3	0.469(9)	489.1	0.445(8)
93.6	2.60(4)	205.8	3.33(5)	588.6	4.51(4)
109.8	17.5(2)	283.2	0.270(3)	593.4	0.048(4)
118.2	1.86(2)	295.9	28.6(3)	604.4	8.19(6)
130.5	11.28(10)	308.4	29.8(3)	612.5	5.31(4)
177.2	22.44(21)	316.5	82.8(7)	884.5	0.295(7)
197.9	36.0(5)	374.5	0.726(12)	1061.5	0.053(3)
240.3	0.1085(12)	416.5	0.667(15)		
261.1	1.68(3)	420.5	0.076(5)		
307.7	10.10(22)	468.1	47.7(4)		

2. Fast Neutron TOF-Spectroscopy and Cross Section Measurements

The energy variable cyclotron and the multi-angle TOF-spectrometer /1/ were used to investigate n-induced reactions on carbon. Some results were presented at the International Conference on "Nuclear Data for Science and Technology" in Antwerp /2, 3, 4/.

2.1 Scattering on Carbon in the Energy Range 6 MeV $\leq E_n \leq$ 14 MeV

R. Böttger, H.J. Brede, H. Klein, H. Schölermann
B.R.L. Siebert

The Monte Carlo code STREUER II which was developed in order to correct for sample size effects has been tested by means of the scattering of 9.9 MeV neutrons on various carbon samples. A full simulation of the TOF-spectra is needed for all samples to describe the position and the shape of the TOF-peaks due to elastic and inelastic scattering on carbon as well as the underlying background originating from multiple neutron scattering /2/.
A new matrix inversion method has been applied which with only one iteration produced a set of Legrendre coefficients to describe the experimental data sufficiently for all samples. The differential cross sections extracted confirmed neither the ENDF/B-V data nor the TUNL-data set.
The analysis of 8 additional data sets between 6 MeV and 14 MeV (ΔE_n = 1 MeV) is in progress.

2.2 Angular distribution of the $^{12}C(n,\alpha)^9Be$ reaction

G. Dietze, H.J. Brede, H. Klein, H. Schölermann

The differential cross section of the reaction $^{12}C(n,\alpha)^9Be$ has been measured in the neutron energy range from 8 MeV to 10 MeV. An NE 213 scintillation detector has been simultaneously used as a carbon target, an α-particle detector and a neutron fluence monitor. Measured and calculated response spectra have been compared in order to separate the fraction of the spectra induced by the reaction $^{12}C(n,\alpha)^{9}Be$. The differential cross section could then be obtained by analyzing the pulse height distribution on the basis of an accurately determined light output function for α-particles in an NE 213 scintillator. The angular distributions vary significantly with the neutron energy and are consistent with data from the inverse reaction $^{9}Be(\alpha,n)^{12}C$ /3/.

The complete data set (ΔE_n = 0.1 MeV) has to be analysed including an estimate of the uncertainties.

2.3 The Neutron Energy Spectrum from the Spontaneous Fission of ^{252}Cf

R. Böttger, H. Klein, A. Chalupka*, B. Strohmaier*

Discrepancies in the description of the neutron energy spectrum of ^{252}Cf above 5 MeV have given rise to an investigation of this part of the spectrum. The new PTB multi-angle neutron time-of-flight spectrometer and an improved version of the IRK low mass ionization chamber were obtained for the measurements. The influence of the detection efficiency for fission fragments on the neutron energy spectrum measured in coincidence with a TOF-detector was carefully studied. The measured spectra were corrected for background due to uncorrelated stops and for the efficiency of the fission chamber. The shape of the spectrum is best described in the energy range 3 MeV $\leq E_n \leq$ 13 MeV by a Maxwellian distribution with the temperature parameter E_o = 1.335 MeV /4/.

*Institut für Radiumforschung und Kernphysik (IRK), Wien

2.4 Monte Carlo Code SINENA

B.R.L. Siebert, H.J. Brede, H. Lesiecki

A Monte Carlo program has been developed which allows the efficiency of proton recoil telescopes (PRT) in realistic neutron fields to be computed. The commonly used direct and indirect methods for calibrating detectors against a PRT have been discussed and generalized for realistic neutron fields which are produced using spatially-extended targets and an anisotropic produced reaction. The gas target using the $D(d,n)^3He$ reaction has been studied as an example of a realistic source. The influence of the entrance foil and the reaction gas have been considered. The correction due to first-order elastic multiple scattering from target material has been implemented. It could be shown that systematic errors of up to 5.5 % can be avoided by the use of the new program as compared to the present standard procedures /5/.

2.5 Monte Carlo Codes NRESP4 and NEFF4

G. Dietze, H. Klein

Two Monte Carlo codes, NRESP4 and NEFF4 were completed to calculate the detector response functions and detections efficiencies for NE 213 scintillation detectors by incidence of fast neutrons in the energy range from 0.02 MeV to 20 MeV. The codes include neutron scattering effects in the aluminum detector housing and in a light pipe. An extensive set of cross section and differential cross section data has been included. Various light output functions for protons may be used /6/.

References

/1/ R. Böttger, H.J. Brede, M. Cosack, G. Dietze, R. Jahr, H. Klein, H. Schölermann, B.R.L. Siebert
Nuclear Data for Science and Technology, p. 836-839, Proc. of the Int. Conf. in Antwerp, ed. K.H. Böckhoff, Reichel Publ. Comp. Dordrecht 1983

/2/ H. Klein, B.R.L. Siebert, R. Böttger, H.J. Brede, H. Schölermann
ibidem, p. 891-894

/3/ G. Dietze, H.J. Brede, H. Klein, H. Schölermann
ibidem, p. 930-933

/4/ R. Böttger, H. Klein, A. Chalupka, B. Strohmaier
ibidem, p. 484-487

/5/ B.R.L. Siebert, H.J. Brede, H. Lesiecki
PTB-report ND-23, Braunschweig, Nov. 82

/6/ G. Dietze, H. Klein
PTB-report ND-22, Braunschweig, Oct. 82

FACHINFORMATIONSZENTRUM ENERGIE PHYSIK MATHEMATIK

Status Report

H. Behrens, J.W. Tepel

1. Information System for Physics Data in the Federal Republic of Germany

This topic has been described earlier in the Progress Reports NEANDC (E) - 172 U Vol. V, NEANDC (E) - 182 U Vol. V and NEANDC (E) - 192 U Vol. V. No details are therefore given here.

2. New Data compilations

The following new issues in the series Physics Data were published in the meantime:

5-16 (1982): Gases and Carbon in Metals (Thermodynamics, Kinetics, and Properties).
Part XVI: Ferrous Metals (4): Iron-Oxygen (Fe-O)
E. Fromm, H. Speck, W. Hehn, H. Jehn and G. Hörz

5-17 (1982): Gases and Carbon in Metals (Thermodynamics, Kinetics, and Properties).
Part XVII: Ferrous Metals (5): Cobalt (Co)
E. Fromm, H. Speck, W. Hehn, H. Jehn and G. Hörz

5-18 (1982): Gases and Carbon in Metals (Thermodynamics, Kinetics, and Properties).
Part XVIII: Ferrous Metals (6): Nickel (Ni)
G. Hörz, H. Speck, E. Fromm and H. Jehn

5-19 (1982): Gases and Carbon in Metals (Thermodynamics, Kinetics, and Properties).
Part XIX: Platinum Metals (1): Palladium (Pd)
H. Jehn, H. Speck, W. Hehn, E. Fromm and G. Hörz

5-2o (1982): Gases and Carbon in Metals (Thermodynamics, Kinetics, and Properties).
Part XX: Platinum Metals (2): Ruthenium, Osmium, Iridium, Platinum (Ru, Rh, Os, Ir, Pt)
H. Jehn, H. Speck, W. Hehn, E. Fromm and G. Hörz

15 (1982):	Karlsruhe Charged Particle Reaction Data Compilation. H. Münzel, H. Klewe-Nebenius, J. Lange, C. Pfennig, K. Hemberle and B. Neumann Loose-leaf collection, LXXVI Supplement to the previous collection published as Nos. 15 (1979)
15-3	Entry 81-11o.XVI
15-4	Entry 111-145.XVI
15-5	Entry 146-18o and CPX-Entry P 1 - P 148.XVI
15-Index	Index to Vol. 1-5 (1982 Edition),XXVIII This issues superseded the previous edition published as No. 15-Index (1979) and includes graphic represen- tations of about 80% of all data sets.
19-1 (1982):	Superconductivity Data. H. Cordes, M. Dietrich, J. Halbritter, H. Hübner, H. von Löhneysen, K. Lüders, R. Meier-Hirmer, U. Poppe, U. Ruppert, W. Schwarz, E. Thorwarth and K. Ullrich VIII
24-1 (1982):	Surface Science Index. 1956-1977. E. Umbach and D. Menzel with the collaboration of H.A. Engelhardt, P. Feulner, R. Franchy, J.C. Fuggle, G. Greiner, R. Jaeger, H. Pfnür, W. Riedl, A. Schischl, V. Schindler et al XII

3. Bibliographie of existing Data Compilations

The bibliographic database "Physcomp" which is relevant for all worldwide existing data compilations in physics is just updated once more. A new printed issue is also in preperation.

4. The Evaluated Nuclear Structure Data File (ENSDF)

The mass chains A=95 and A=96 have been published or will soon be issued. The mass chain A=98 is in the review procedure. At the moment the mass chains A=92, 93, 94, 97 and 99 are in preparation, whereby some of these are in an advanced stage.

The three nuclear structure relevant databases ENSDF, NSR (Nuclear Structure Reference File) and MEDLIST (containing the radiation emitted from all unstable nucleides) have been implemented as ADABAS files on our Siemens 7.561 computer. They are now offered for online-access via networks on a regular basis. A description is available on request.

APPENDIX

Adresses of Contributing Laboratories

Institut für Angewandte Kernphysik II
Director: Prof.Dr. G. Schatz
Senior reporter: Dr. F. Käppeler
Kernforschungszentrum Karlsruhe
Postfach 3640
7500 Karlsruhe

Institut für Kernphysik II
Director: Prof.Dr. A. Citron
Senior reporter: Dr. S. Cierjacks
Kernforschungszentrum Karlsruhe
Postfach 3640
7500 Karlsruhe

Institut für Neutronenphysik und Reaktortechnik
Director: Prof.Dr. G. Kessler
Senior reporter: Dr. F.H. Fröhner
Kernforschungszentrum Karlsruhe
Postfach 3640
7500 Karlsruhe

Institut für Chemie (1): Nuklearchemie
Director: Prof.Dr. G. Stöcklin
Senior reporter: Dr. S.M. Qaim
Kernforschungsanlage Jülich
Postfach 1913
5170 Jülich

I. Institut für Experimentalphysik
Director: Prof.Dr. H. Brückmann
Senior reporter: Prof.Dr. W. Scobel
Universität Hamburg
Luruper Chaussee 149
2000 Hamburg 50

Institut für Reine und Angewandte
Kernphysik
Director: Prof.Dr. K.O. Thielheim
Senior reporter: Dr. H.-G. Priesmeyer
Universität Kiel, Geesthacht
Reaktorstr. 1
2054 Geesthacht/Tesperhude

Institut für Kernchemie
Director: Prof.Dr. W. Herr
Senior reporter: Dr. R. Michel
Universität zu Köln
Zülpicher Str. 47
5000 Köln

Institut für Kernchemie
Director: Prof.Dr. G. Herrmann
Senior reporter: Prof.Dr. H.O. Denschlag
Universität Mainz
Fritz-Strassmann-Weg 2
6500 Mainz

Institut für Kernchemie
Senior reporter: Prof.Dr. P. Patzelt
Philipps-Universität Marburg
Lahnberge
3550 Marburg/Lahn

Fachbereich Physik der
Technischen Universität München
Abteilung E14, Forschungsreaktor
Head and senior reporter: Prof.Dr. L. Köster
8046 Garching/München

Institut für Kernenergetik und Energiesysteme
Director: Prof.Dr. K.H. Höcker
Senior reporter: Dr. J. Keinert
Universität Stuttgart
Pfaffenwaldring 31
7000 Stuttgart 80 (Vaihingen)

Institut für Strahlenphysik
Director: Prof.Dr. K.W. Hoffmann
Senior reporter: J.W. Hammer
Universität Stuttgart
Allmandring 3
7000 Stuttgart 80

Physikalisch-Technische Bundesanstalt
Abteilung 6, Atomphysik
Director: Prof.Dr. S. Wagner
Bundesallee 100
3300 Braunschweig

Fachinformationszentrum Energie, Physik, Mathematik
Directors: Dr. W. Rittberger, E.-O. Schulze
Senior reporter: Dr. H. Behrens
Kernforschungszentrum
7514 Eggenstein-Leopoldshafen 2

ELEMENT S	A	QUANTITY	TYPE	ENERGY MIN	MAX	DOCUMENTATION REF	VOL	PAGE	DATE	LAB	COMMENTS
MA	NY	N,HELIUM3	EXPT-PROG	FAST		NEANDC(E)-242U			683	JUL	VOL.5.P.24 QAIM+ NHE3/NHE4 SIG RATIO
H	001	THERMAL SCAT	EXPT-PROG	40-2	10+0	NEANDC(E)-242U			683	KIG	VOL.5.P.33 PRIESMEYER+ (N,P) IN ZRH
LI	006	THERMAL SCAT	EXPT-PROG	SLOW		NEANDC(E)-242U			683	MUN	VOL.5.P.51 KOESTER+ SCAT LENGTHS
LI	007	N,N TRITON	EXPT-PROG	13+7	16+7	NEANDC(E)-242U			683	JUL	VOL.5.P.26 LISKIEN+ SIG, NDG
LI	007	THERMAL SCAT	EXPT-PROG	SLOW		NEANDC(E)-242U			683	MUN	VOL.5.P.51 KOESTER+ SCAT LENGTHS
B	010	THERMAL SCAT	EXPT-PROG	SLOW		NEANDC(E)-242U			683	MUN	VOL.5.P.51 KOESTER+ SCAT LENGTHS
B	011	THERMAL SCAT	EXPT-PROG	SLOW		NEANDC(E)-242U			683	MUN	VOL.5.P.51 KOESTER+ SCAT LENGTHS
C		SCATTERING	THEO-PROG	60+6	14+7	NEANDC(E)-242U			683	PTB	VOL.5.P.65 BOETTGER+ EXPT DATA ANAL
C	012	N,ALPHA	EXPT-PROG	80+6	10+7	NEANDC(E)-242U			683	PTB	VOL.5.P.65 DIETZE+ ANGDIST,NDG
NE	020	N,GAMMA	EXPT-PROG	50+3	40+5	NEANDC(E)-242U			683	KFK	VOL.5.P.1.ALMEIDA+ ABST,NDG
NE	020	N,GAMMA	EXPT-PROG	30+4		NEANDC(E)-242U			683	KFK	VOL.5.P.1 ALMEIDA+ MAXW AVG SIG,NDG
NE	020	TOT	EXPT-PROG	50+3	80+5	NEANDC(E)-242U			683	KFK	VOL.5.P.1.ALMEIDA+ ABST,NDG
NE	021	N,GAMMA	EXPT-PROG	50+3	40+5	NEANDC(E)-242U			683	KFK	VOL.5.P.1.ALMEIDA ABST,NDG
NE	021	N,GAMMA	EXPT-PROG	30+4		NEANDC(E)-242U			683	KFK	VOL.5.P.1 ALMEIDA+ MAXW AVG SIG,NDG
NE	021	TOT	EXPT-PROG	50+3	80+5	NEANDC(E)-242U			683	KFK	VOL.5.P.1.ALMEIDA+ ABST,NDG
NE	022	N,GAMMA	EXPT-PROG	50+3	40+5	NEANDC(E)-242U			683	KFK	VOL.5.P.1.ALMEIDA+ ABST,NDG
NE	022	N,GAMMA	EXPT-PROG	30+4		NEANDC(E)-242U			683	KFK	VOL.5.P.1 ALMEIDA+ MAXW AVG SIG,NDG
NE	022	TOT	EXPT-PROG	50+3	80+5	NEANDC(E)-242U			683	KFK	VOL.5.P.1.ALMEIDA+ ABST,NDG
AL	027	N,ALPHA	EXPT-PROG	63+6	83+6	NEANDC(E)-242U			683	THS	VOL.5.P.58 ENZ+ ACT METHOD,GRPH,TBL
SI		POLARIZATION	EXPT-PROG	78+6		NEANDC(E)-242U			683	THS	VOL.5.P.60 BULSKI+ ANALYZING POWER
S		POLARIZATION	EXPT-PROG	78+6		NEANDC(E)-242U			683	THS	VOL.5.P.60 BULSKI+ ANALYZING POWER
CA		POLARIZATION	EXPT-PROG	78+6		NEANDC(E)-242U			683	THS	VOL.5.P.60 BULSKI+ ANALYZING POWER
FE	056	N,GAMMA	EXPT-PROG	10+4	25+5	NEANDC(E)-242U			683	KFK	VOL.5.P.2 KAEPPELER+ REL AU,ABST,NDG
FE	056	RESON PARAMS	EXPT-PROG	10+4	10+5	NEANDC(E)-242U			683	KFK	VOL.5.P.2 KAEPPELER+ RESPARS,NDG
FE	056	RESON PARAMS	EXPT-PROG	28+4		NEANDC(E)-242U			683	KFK	VOL.5.P.3 WISSHAK+ WG, S-WAVE
FE	058	N,GAMMA	EXPT-PROG	10+4	25+5	NEANDC(E)-242U			683	KFK	VOL.5.P.2 KAEPPELER+ REL AU,ABST,NDG
FE	058	RESON PARAMS	EXPT-PROG	10+4	10+5	NEANDC(E)-242U			683	KFK	VOL.5.P.2 KAEPPELER+ RESPARS,NDG
NI	058	N,ALPHA	EXPT-PROG	40+6	90+6	NEANDC(E)-242U			683	JUL	VOL.5.P.25 QAIM+ EXCITATION FN, NDG
NI	058	RESON PARAMS	EXPT-PROG	15+4		NEANDC(E)-242U			683	KFK	VOL.5.P.3 WISSHAK+ WG, S-WAVE
NI	060	RESON PARAMS	EXPT-PROG	13+4		NEANDC(E)-242U			683	KFK	VOL.5.P.3 WISSHAK+ WG, S-WAVE
NI	061	N,PROTON	EXPT-PROG	40+6	90+6	NEANDC(E)-242U			683	JUL	VOL.5.P.25 QAIM+ EXCITATION FN, NDG
NI	062	N,ALPHA	EXPT-PROG	40+6	90+6	NEANDC(E)-242U			683	JUL	VOL.5.P.25 QAIM+ EXCITATION FN, NDG
NI	062	N,PROTON	EXPT-PROG	40+6	90+6	NEANDC(E)-242U			683	JUL	VOL.5.P.25 QAIM+ EXCITATION FN, NDG
NI	064	N,GAMMA	EXPT-PROG	10+4	55+4	NEANDC(E)-242U			683	KFK	VOL.5.P.4 WISSHAK+ GRAPHS,FANAC FIT

NI 064	RESON PARAMS	EXPT-PROG	14+4 34+4	NEANDC(E)-242U 683 KFK	VOL.5.P.4 WISSHAK+ WG,S-WAVE
GA	THERMAL SCAT	EXPT-PROG	SLOW	NEANDC(E)-242U 683 MUN	VOL.5.P.52 KOESTER+ MELT,SCAT LENGTH
GA 071	N,GAMMA	EXPT-PROG	25+4	NEANDC(E)-242U 683 KFK	VOL.5.P.7 WALTER+ ACT METHOD,NDG
AS 075	N,GAMMA	EXPT-PROG	25+4	NEANDC(E)-242U 683 KFK	VOL.5.P.7 WALTER+ ACT METHOD,NDG
BR 079	N,GAMMA	EXPT-PROG	25+4	NEANDC(E)-242U 683 KFK	VOL.5.P.7 WALTER+ ACT METHOD,NDG
BR 081	N,GAMMA	EXPT-PROG	25+4	NEANDC(E)-242U 683 KFK	VOL.5.P.7 WALTER+ ACT METHOD,NDG
KR 080	N,GAMMA	EXPT-PROG	30+4	NEANDC(E)-242U 683 KFK	VOL.5.P.6 WALTER+ MAXW AVG SIG, NDG
KR 080	N,GAMMA	EXPT-PROG	40+3 29+5	NEANDC(E)-242U 683 KFK	VOL.5.P.6 WALTER+ ABST,NDG
KR 084	N,GAMMA	EXPT-PROG	25-2	NEANDC(E)-242U 683 KFK	VOL.5.P.6 PENZHORN+ ACT METHOD, NDG
KR 084	N,GAMMA	EXPT-PROG	25+4	NEANDC(E)-242U 683 KFK	VOL.5.P.6 PENZHORN+ ACT METHOD, NDG
KR 086	N,GAMMA	EXPT-PROG	25+4	NEANDC(E)-242U 683 KFK	VOL.5.P.7 WALTER+ ACT METHOD,NDG
RB 085	N,GAMMA	EXPT-PROG	25+4	NEANDC(E)-242U 683 KFK	VOL.5.P.7 WALTER+ ACT METHOD,NDG
RB 087	N,GAMMA	EXPT-PROG	25+4	NEANDC(E)-242U 683 KFK	VOL.5.P.7 WALTER+ ACT METHOD,NDG
Y	POLARIZATION	EXPT-PROG	78+6	NEANDC(E)-242U 683 THS	VOL.5.P.60 BULSKI+ ANALYZING POWER
SN	THERMAL SCAT	EXPT-PROG	SLOW	NEANDC(E)-242U 683 MUN	VOL.5.P.52 KOESTER+ MELT,SCAT LENGTH
XE 124	N,GAMMA	EXPT-PROG	25+4	NEANDC(E)-242U 683 KFK	VOL.5.P.7 BEER+ ACT METHOD, NDG
XE 128	N,GAMMA	THEO-PROG	25+4	NEANDC(E)-242U 683 KFK	VOL.5.P.7 BEER+ STATMODL CALC, NDG
XE 129	N,GAMMA	THEO-PROG	25+4	NEANDC(E)-242U 683 KFK	VOL.5.P.7 BEER+ STATMODL CALC, NDG
XE 130	N,GAMMA	THEO-PROG	25+4	NEANDC(E)-242U 683 KFK	VOL.5.P.7 BEER+ STATMODL CALC, NDG
XE 131	N,GAMMA	THEO-PROG	25+4	NEANDC(E)-242U 683 KFK	VOL.5.P.7 BEER+ STATMODL CALC, NDG
XE 132	N,GAMMA	EXPT-PROG	25+4	NEANDC(E)-242U 683 KFK	VOL.5.P.7 BEER+ ACT METHOD, NDG
XE 134	N,GAMMA	EXPT-PROG	25+4	NEANDC(E)-242U 683 KFK	VOL.5.P.7 BEER+ ACT METHOD, NDG
LA	POLARIZATION	EXPT-PROG	87+6	NEANDC(E)-242U 683 THS	VOL.5.P.60 BULSKI+ ANALYZING POWER
LA	THERMAL SCAT	EXPT-PROG	SLOW	NEANDC(E)-242U 683 MUN	VOL.5.P.51 KNOPF+ SCAT LENGTHS

ELEMENT S	A	QUANTITY	TYPE	ENERGY MIN	MAX	DOCUMENTATION REF	VOL	PAGE	DATE	LAB	COMMENTS
CE		THERMAL SCAT	EXPT-PROG	SLOW		NEANDC(E)-242U			683	MUN	VOL.5.P.51 KNOPF+ SCAT LENGTHS
CE	136	THERMAL SCAT	EXPT-PROG	SLOW		NEANDC(E)-242U			683	MUN	VOL.5.P.51 KNOPF+ SCAT LENGTHS
CE	138	THERMAL SCAT	EXPT-PROG	SLOW		NEANDC(E)-242U			683	MUN	VOL.5.P.51 KNOPF+ SCAT LENGTHS
CE	140	THERMAL SCAT	EXPT-PROG	SLOW		NEANDC(E)-242U			683	MUN	VOL.5.P.51 KNOPF+ SCAT LENGTHS
CE	142	THERMAL SCAT	EXPT-PROG	SLOW		NEANDC(E)-242U			683	MUN	VOL.5.P.51 KNOPF+ SCAT LENGTHS
ND	142	N,GAMMA	EXPT-PROG	30+4		NEANDC(E)-242U			683	KFK	VOL.5.P.7 MATHEWS+ MAXW AVG SIG
ND	142	N,GAMMA	EXPT-PROG	60+3	25+5	NEANDC(E)-242U			683	KFK	VOL.5.P.7 MATHEWS+ NDG
ND	143	N,GAMMA	EXPT-PROG	30+4		NEANDC(E)-242U			683	KFK	VOL.5.P.7 MATHEWS+ MAXW AVG SIG
ND	143	N,GAMMA	EXPT-PROG	60+3	25+5	NEANDC(E)-242U			683	KFK	VOL.5.P.7 MATHEWS+ NDG
ND	144	N,GAMMA	EXPT-PROG	30+4		NEANDC(E)-242U			683	KFK	VOL.5.P.7 MATHEWS+ MAXW AVG SIG
ND	144	N,GAMMA	EXPT-PROG	60+3	25+5	NEANDC(E)-242U			683	KFK	VOL.5.P.7 MATHEWS+ NDG
ND	147	N,GAMMA	THEO-PROG	10+3	10+5	NEANDC(E)-242U			683	KFK	VOL.5.P.8 WINTERS+ H-F CALC,TBL
ND	147	N,GAMMA	THEO-PROG	30+4		NEANDC(E)-242U			683	KFK	VOL.5.P.8 WINTERS+MAXW AVG,H-F CALC
PM	147	N,GAMMA	THEO-PROG	10+3	10+5	NEANDC(E)-242U			683	KFK	VOL.5.P.8 WINTERS+ H-F CALC,TBL
PM	147	N,GAMMA	THEO-PROG	30+4		NEANDC(E)-242U			683	KFK	VOL.5.P.8 WINTERS+MAXW AVG,H-F CALC
PM	148	N,GAMMA	THEO-PROG	10+3	10+5	NEANDC(E)-242U			683	KFK	VOL.5.P.8 WINTERS+ H-F CALC,TBL
PM	148	N,GAMMA	THEO-PROG	30+4		NEANDC(E)-242U			683	KFK	VOL.5.P.8 WINTERS+MAXW AVG,H-F CALC
SM	148	N,GAMMA	EXPT-PROG	30+4		NEANDC(E)-242U			683	KFK	VOL.5.P.8 WINTERS+ MAXW AVG SIG
SM	148	N,GAMMA	EXPT-PROG	40+3	25+5	NEANDC(E)-242U			683	KFK	VOL.5.P.8 WINTERS+ NDG
SM	149	N,GAMMA	EXPT-PROG	30+4		NEANDC(E)-242U			683	KFK	VOL.5.P.8 WINTERS+ MAXW AVG SIG
SM	149	N,GAMMA	EXPT-PROG	40+3	25+5	NEANDC(E)-242U			683	KFK	VOL.5.P.8 WINTERS+ NDG
SM	150	N,GAMMA	EXPT-PROG	30+4		NEANDC(E)-242U			683	KFK	VOL.5.P.8 WINTERS+ MAXW AVG SIG
SM	150	N,GAMMA	EXPT-PROG	40+3	25+5	NEANDC(E)-242U			683	KFK	VOL.5.P.8 WINTERS+ NDG
SM	151	N,GAMMA	THEO-PROG	10+3	10+5	NEANDC(E)-242U			683	KFK	VOL.5.P.8 WINTERS+ H-F CALC,TBL
SM	151	N,GAMMA	THEO-PROG	30+4		NEANDC(E)-242U			683	KFK	VOL.5.P.8 WINTERS+MAXW AVG,H-F CALC
HF	178	N,GAMMA	EXPT-PROG	26+3	20+6	NEANDC(E)-242U			683	KFK	VOL.5.P.10 BEER+ ABST,NDG
HF	178	RESON PARAMS	EXPT-PROG	26+3	10+4	NEANDC(E)-242U			683	KFK	VOL.5.P.10 BEER+ ABST,NDG
HF	179	N,GAMMA	EXPT-PROG	26+3	20+6	NEANDC(E)-242U			683	KFK	VOL.5.P.10 BEER+ ABST,NDG
HF	179	RESON PARAMS	EXPT-PROG	26+3	10+4	NEANDC(E)-242U			683	KFK	VOL.5.P.10 BEER+ ABST,NDG
HF	180	N,GAMMA	EXPT-PROG	26+3	20+6	NEANDC(E)-242U			683	KFK	VOL.5.P.10 BEER+ ABST,NDG
HF	180	RESON PARAMS	EXPT-PROG	26+3	10+4	NEANDC(E)-242U			683	KFK	VOL.5.P.10 BEER+ ABST,NDG
HG	198	N,GAMMA	EXPT-PROG	25+5		NEANDC(E)-242U			683	KFK	VOL.5.P.11 WALTER+ ACT METHOD
TL		THERMAL SCAT	EXPT-PROG	SLOW		NEANDC(E)-242U			683	MUN	VOL.5.P.52 KOESTER+ MELT,SCAT LENGTH
PB		THERMAL SCAT	EXPT-PROG	SLOW		NEANDC(E)-242U			683	MUN	VOL.5.P.52 KOESTER+ MELT,SCAT LENGTH
BI		THERMAL SCAT	EXPT-PROG	SLOW		NEANDC(E)-242U			683	MUN	VOL.5.P.52 KOESTER+ MELT,SCAT LENGTH
U		TOTAL	EXPT-PROG	30+0	14+2	NEANDC(E)-242U			683	KIG	VOL.5.P.34 PRIESMEYER+ TRANSM EXPT
U	235	FISS PROD G	EXPT-PROG	PILE		NEANDC(E)-242U			683	MNZ	VOL.5.P.47 SOHNIUS+ MASS 144,146,147
AM	243	EVALUATION	EXPT-PROG	30+3	30+5	NEANDC(E)-242U			683	KFK	VOL.5.P.21 FROEHNER+NF FIT,EXPT DATA
AM	243	N,FISSION	EXPT-PROG	30+3	30+5	NEANDC(E)-242U			683	KFK	VOL.5.P.21 FROEHNER+ EXPT DATA FIT
AM	243	N,FISSION	EXPT-PROG	50+3	25+5	NEANDC(E)-242U			683	KFK	VOL.5.P.12 WISSHAK+ ABST,NDG
AM	243	N,GAMMA	EXPT-PROG	50+3	25+5	NEANDC(E)-242U			683	KFK	VOL.5.P.12 WISSHAK+ ABST,NDG
CF	252	SPECT FISS N	EXPT-PROG	SPON		NEANDC(E)-242U			683	PTB	VOL.5.P.66 BOETTGER+ N-EN SPEC,NDG